Dynamical description of strongly interacting matter at finite temperature and baryon-chemical potential

Elena Bratkovskaya

for the PHSD group

(GSI Darmstadt & Uni. Frankfurt)

Observables of Hadronization and the QCD Phase Diagram in the Cross-over Domain,
ECT*, Trento, 15 - 19 October 2018

The ‚holy grail‘ of heavy-ion physics:

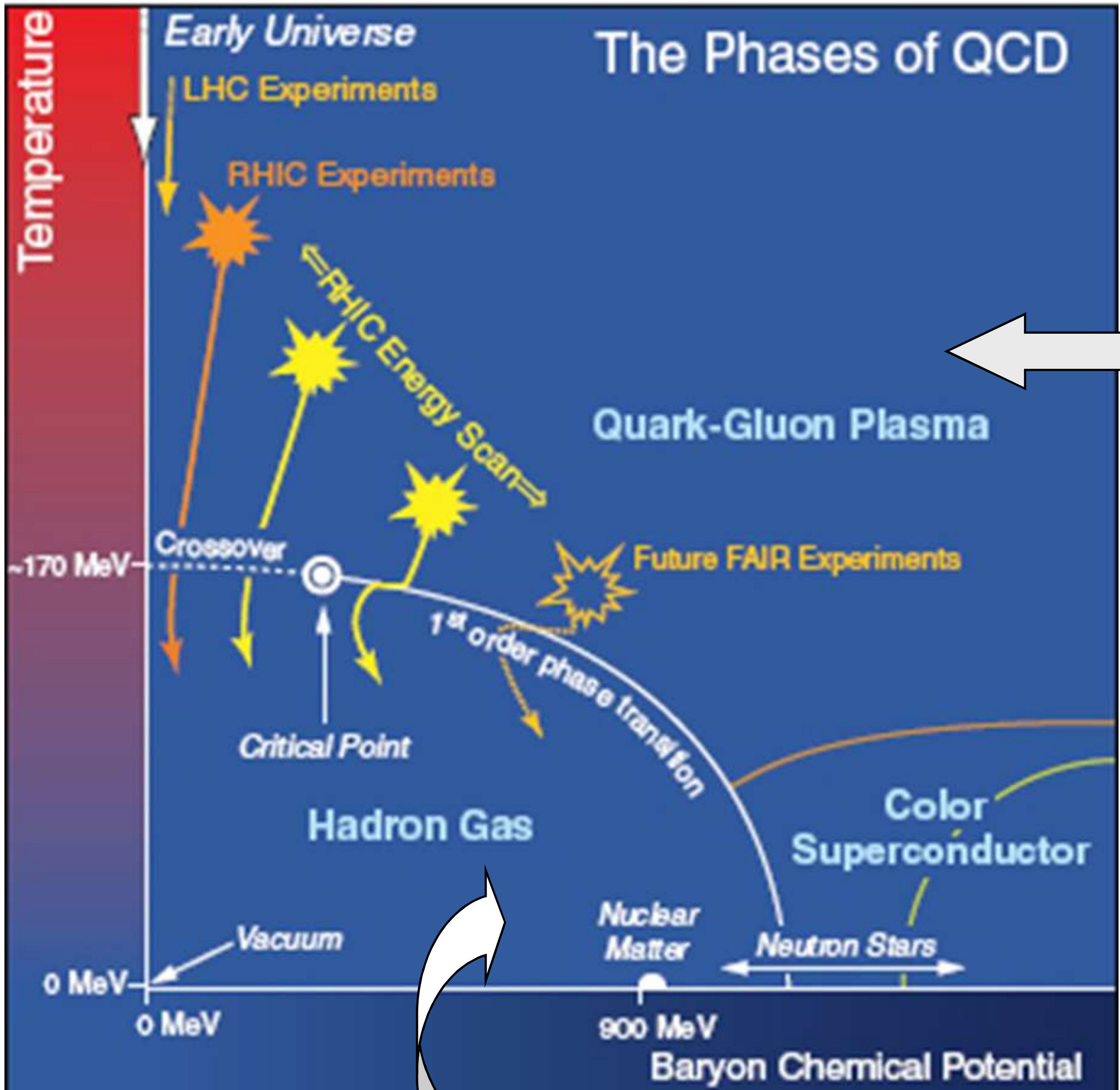

The phase diagram of QCD

- Study of the phase transition from hadronic to partonic matter – Quark-Gluon-Plasma

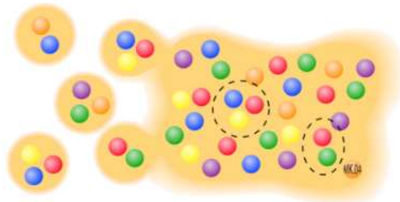

- Search for the critical point
- Search for signatures of chiral symmetry restoration
- Study of the in-medium properties of hadrons at high baryon density and temperature

Theory: Information from lattice QCD

I. deconfinement phase transition with increasing temperature **+** **II. chiral symmetry restoration** with increasing temperature

lQCD BMW collaboration: $\mu_q=0$

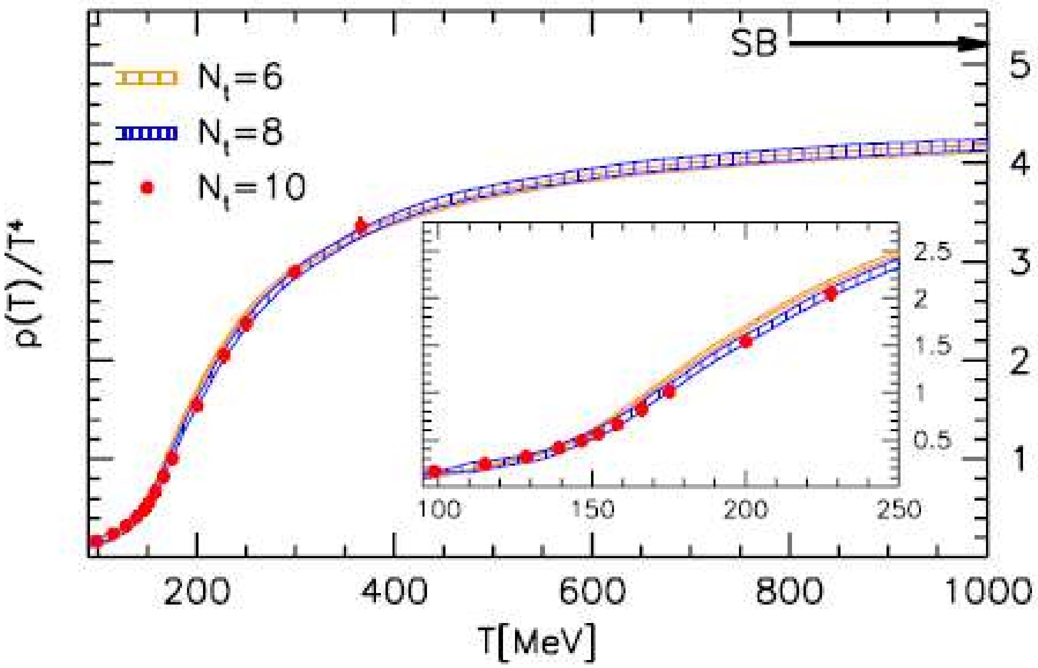

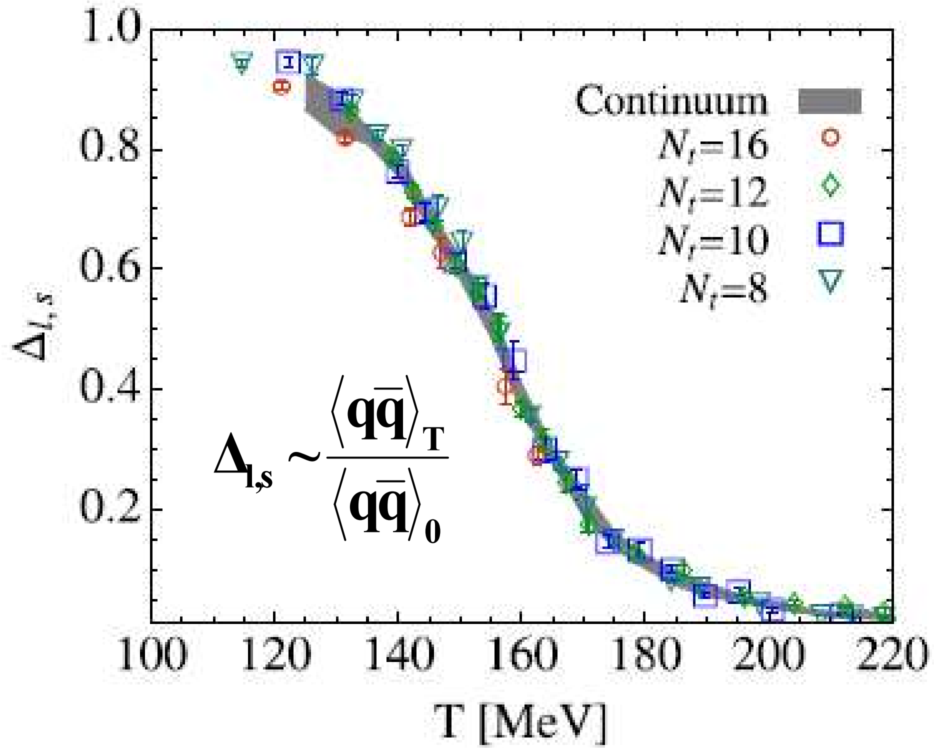

- **Crossover: hadron gas → QGP**
- **Scalar quark condensate $\langle q\bar{q}\rangle$ is viewed as an order parameter for the restoration of chiral symmetry:**

$$< \bar{q}q >= \begin{cases} \neq 0 & \text{chiral non-symmetric phase;} \\ = 0 & \text{chiral symmetric phase.} \end{cases}$$

➔ **both transitions occur at about the same temperature T_C for low chemical potentials**

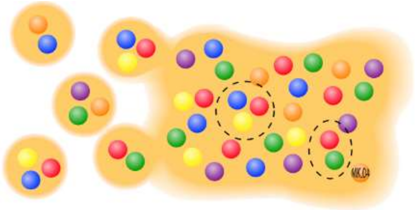

Degrees-of-freedom of QGP

❖ lQCD gives QGP EoS at finite μ_B

! need to be interpreted in terms of degrees-of-freedom

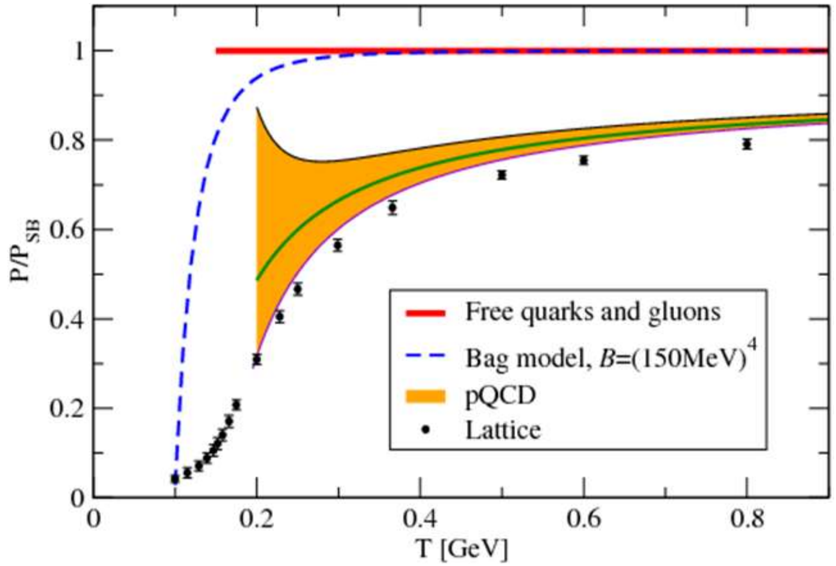

Non-perturbative QCD ← pQCD

Thermal QCD
= QCD at high parton densities:

pQCD:

- ❑ weakly interacting system
- ❑ massless quarks and gluons

- ❑ strongly interacting system
- ❑ massive quarks and gluons

➔ quasiparticles
= effective degrees-of-freedom

❖ How to learn about degrees-of-freedom of QGP ? ➔ HIC experiments

Dynamical QuasiParticle Model (DQPM) - Basic ideas:

DQPM describes QCD properties in terms of 'resummed' single-particle Green's functions (propagators) – in the sense of a two-particle irreducible (2PI) approach:

gluon propagator: $\Delta^{-1} = P^2 - \Pi$ & quark propagator $S_q^{-1} = P^2 - \Sigma_q$

gluon self-energy: $\Pi = M_g^2 - i2\gamma_g\omega$ & quark self-energy: $\Sigma_q = M_q^2 - i2\gamma_q\omega$

(scalar approximation)

- the resummed properties are specified by complex (retarded) self-energies:
  - the real part of self-energies (Σ_q, Π) describes a dynamically generated mass (M_q,M_g);
  - the imaginary part describes the interaction width of partons (γ_q, γ_g)
  - Spectral functions : $A_q \sim Im S_q^{ret}, \quad A_g \sim Im\Delta^{ret}$

- Entropy density of interacting bosons and fermions in the quasiparticle limit (2PI) (G. Baym 1998):

QGP

$$s^{dqp} = -d_g \int \frac{d\omega}{2\pi}\frac{d^3p}{(2\pi)^3}\frac{\partial n_B}{\partial T}\left(\mathrm{Im}\ln(-\Delta^{-1}) + \mathrm{Im}\,\Pi\,\mathrm{Re}\,\Delta\right) \quad \text{gluons}$$

$$- d_q \int \frac{d\omega}{2\pi}\frac{d^3p}{(2\pi)^3}\frac{\partial n_F((\omega-\mu_q)/T)}{\partial T}\left(\mathrm{Im}\ln(-S_q^{-1}) + \mathrm{Im}\,\Sigma_q\,\mathrm{Re}\,S_q\right) \quad \text{quarks}$$

$$- d_{\bar q} \int \frac{d\omega}{2\pi}\frac{d^3p}{(2\pi)^3}\frac{\partial n_F((\omega+\mu_q)/T)}{\partial T}\left(\mathrm{Im}\ln(-S_{\bar q}^{-1}) + \mathrm{Im}\,\Sigma_{\bar q}\,\mathrm{Re}\,S_{\bar q}\right) \quad \text{antiquarks}$$

A. Peshier, W. Cassing, PRL 94 (2005) 172301; Cassing, NPA 791 (2007) 365: NPA 793 (2007)

DQPM (T)

DQPM(T): properties of quasiparticles

Properties of **interacting quasi-particles:**
massive quarks and gluons (g, q, q_{bar})
with **Lorentzian spectral functions :**

$$A(\omega, \boldsymbol{p}) = \frac{\gamma}{E}\left(\frac{1}{(\omega-E)^2+\gamma^2} - \frac{1}{(\omega+E)^2+\gamma^2}\right)$$

$$E^2 = p^2 + M^2 - \gamma^2$$

- Modeling of the quark/gluon masses and widths → HTL limit at high T

masses: $m_g^2 = \frac{g^2}{6}\left(N_c + \frac{1}{2}N_f\right)T^2 , \qquad m_q^2 = g^2 \frac{N_c^2-1}{8N_c} T^2$

widths: $\gamma_g = \frac{1}{3}N_c \frac{g^2 T}{8\pi} \ln\left(\frac{2c}{g^2}+1\right) , \quad \gamma_q = \frac{1}{3}\frac{N_c^2-1}{2N_c}\frac{g^2 T}{8\pi}\ln\left(\frac{2c}{g^2}+1\right)$

- **running coupling** (pure glue):

$$\alpha_s(T) = \frac{g^2(T)}{4\pi} = \frac{12\pi}{(11N_c - 2N_f)\ln[\lambda^2(T/T_c - T_s/T_c)^2]}$$

❑ **fit to lattice (lQCD) results** (e.g. entropy density)

with 3 parameters: T_s/T_c=0.46; c=28.8; λ=2.42 (for pure glue N_f=0)

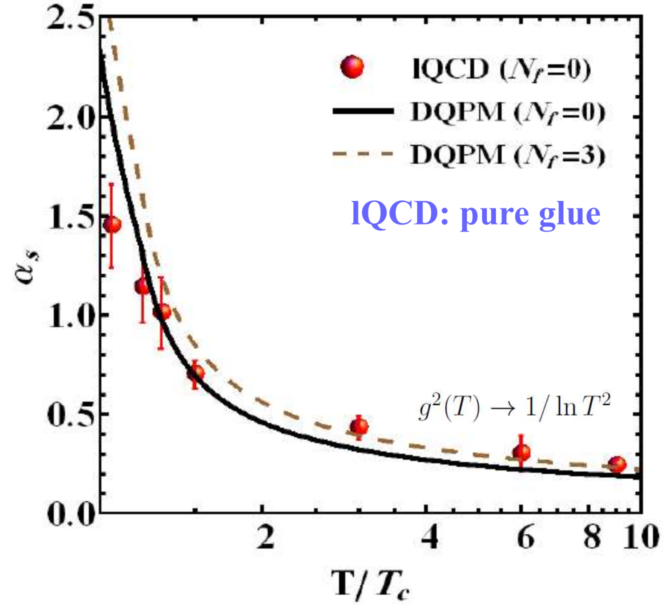

Peshier, Cassing, PRL 94 (2005) 172301;
Cassing, NPA 791 (2007) 365: NPA 793 (2007)

DQPM at finite T and μ_q=0

- **fit to lattice (lQCD) results**
  - * **BMW lQCD data S. Borsanyi et al., JHEP 1009 (2010) 073**

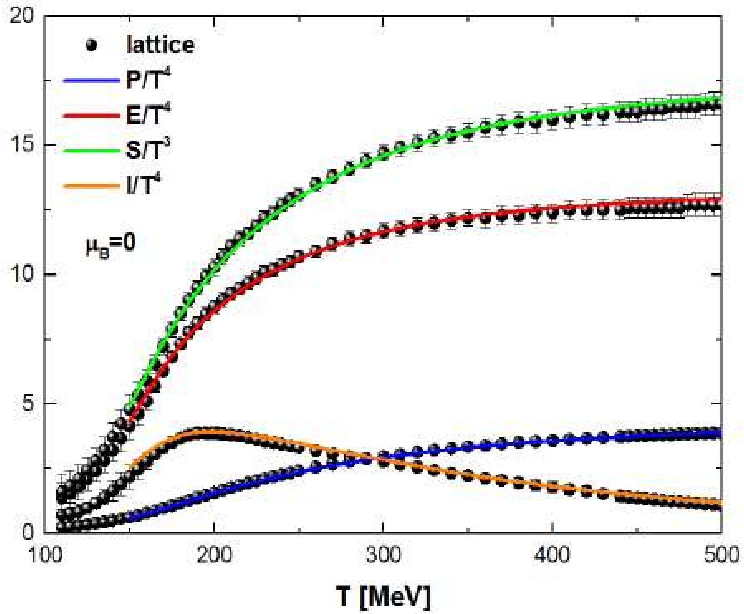

→ Quasiparticle properties:

- **large width and mass for gluons and quarks**

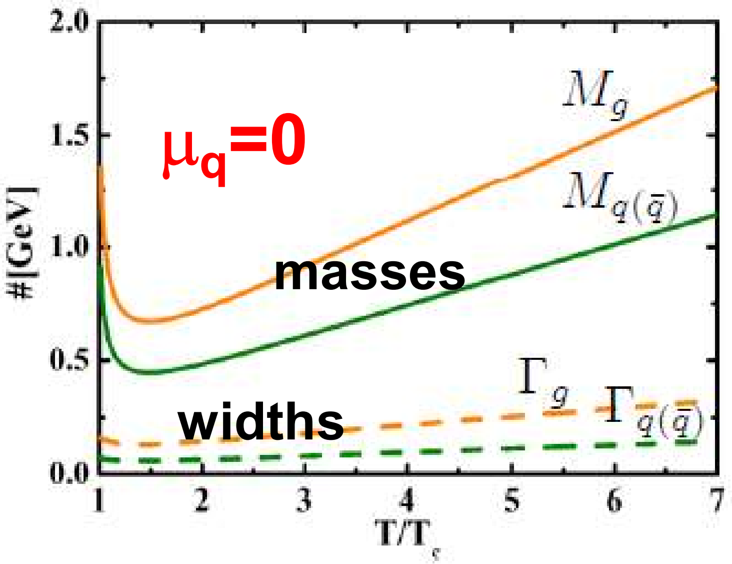

M~gT

T_C=158 MeV
ε_C=0.5 GeV/fm^3

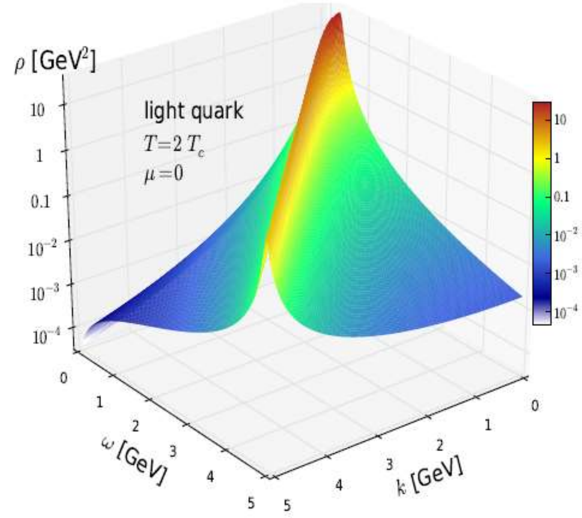

DQPM

- **matches well lattice QCD**
- **provides mean-fields (1PI) for gluons and quarks – from space-like part of $T_{\mu\nu}$ as well as effective 2-body interactions (2PI)**
- **gives transition rates for the formation of hadrons**

→ microscopic dynamical transport approach PHSD

Peshier, Cassing, PRL 94 (2005) 172301; Cassing, NPA 791 (2007) 365: NPA 793 (2007)

Traces of the QGP in observables in high energy heavy-ion collisions

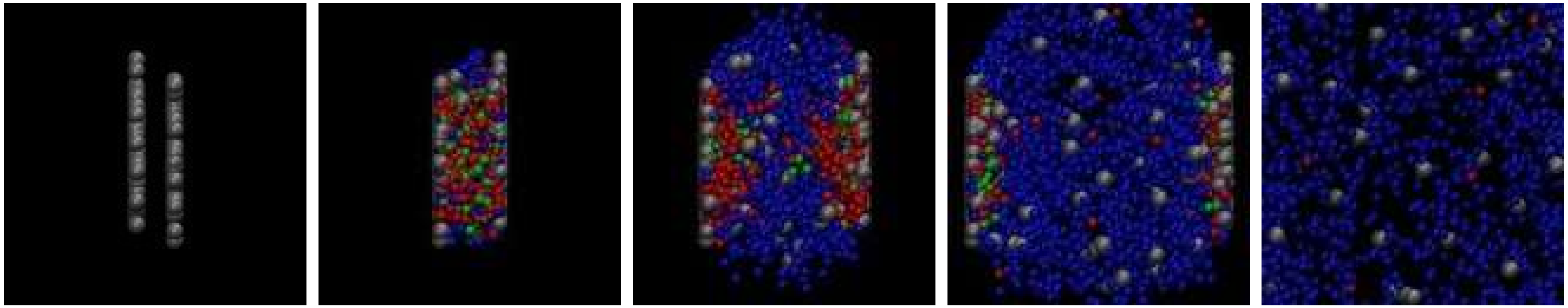

http://theory.gsi.de/~ebratkov/phsd-project/PHSD/index1.html

Basic idea: off-shell PHSD approach

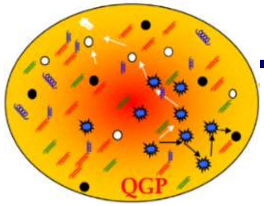

QGP in equilibrium

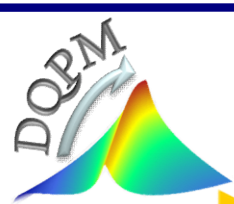

Dynamical QuasiParticle Model (DQPM):

fitted to

lQCD

controled by lQCD!

Quasiparticle properties:
‚resummed' self-energies, propagators
➔ Calculation of cross sections

Calculation of transport coefficients in equilibrium $\eta, \zeta, \sigma_0, ..$

DQPM: consider the effects of the nonperturbative nature of the strongly interacting quark-gluon plasma (sQGP) constituents (vs. pQCD models)

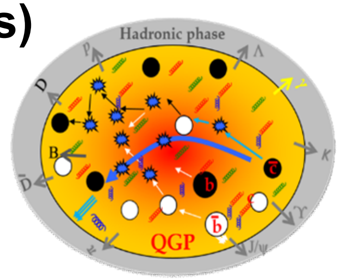

QGP out-of equilibrium ⇔ HIC

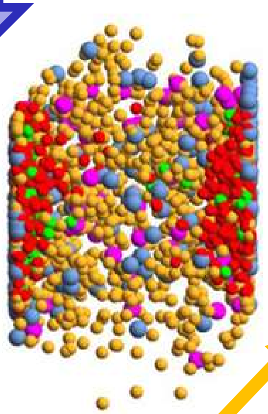

Parton-Hadron-String-Dynamics (PHSD)

controlled by

experimental data + lQCD

Presently - DQPM (T)

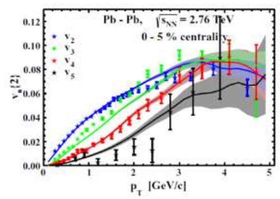

Partonic interactions → DQPM
hadronic interactions → hadron physics
* In-medium hadronic interactions → many-body physics: G-matrix

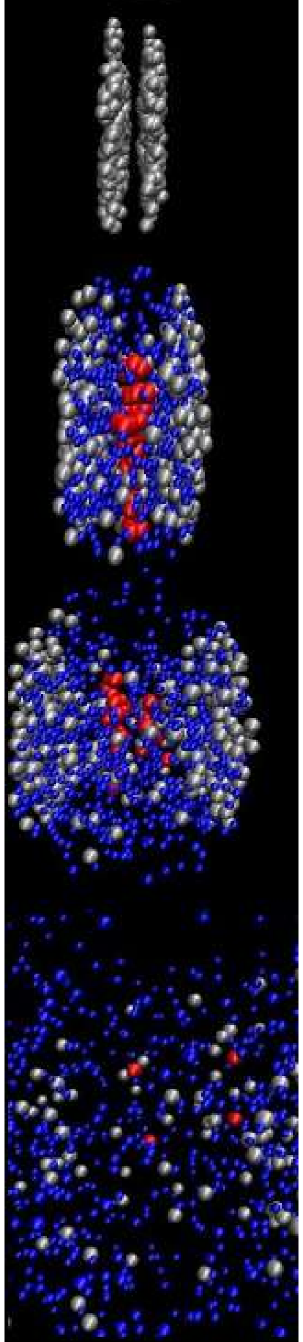

Parton-Hadron-String-Dynamics (PHSD)

- **Initial A+A collisions** :
  N+N → string formation → decay to pre-hadrons

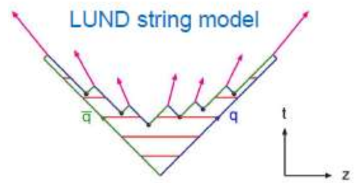

- **Formation of QGP stage** if $\varepsilon > \varepsilon_{critical}$:
  dissolution of pre-hadrons → (DQPM) →
  → massive quarks/gluons + mean-field potential U_q

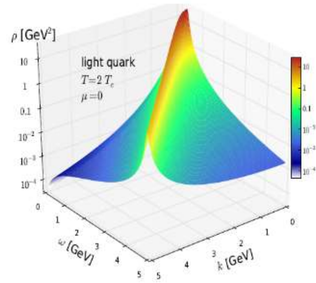

- **Partonic stage – QGP** :
  based on the Dynamical Quasi-Particle Model (DQPM)

  - (quasi-) elastic collisions:

$$q+q \to q+q \qquad g+q \to g+q$$
$$q+\bar{q} \to q+\bar{q} \qquad g+\bar{q} \to g+\bar{q}$$
$$\bar{q}+\bar{q} \to \bar{q}+\bar{q} \qquad g+g \to g+g$$

  - inelastic collisions:

$$q+\bar{q} \to g \qquad q+\bar{q} \to g+g$$
$$g \to q+\bar{q} \qquad g \to g+g$$

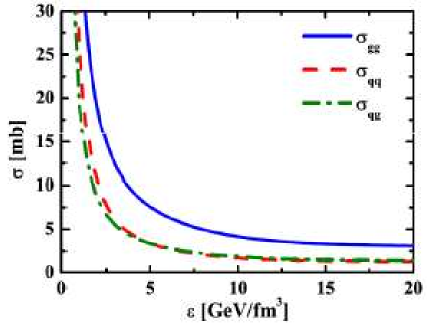

- **Hadronization** (based on DQPM):

$$g \to q+\bar{q}, \qquad q+\bar{q} \leftrightarrow meson \ (or\ 'string')$$
$$q+q+q \leftrightarrow baryon \ (or\ 'string')$$

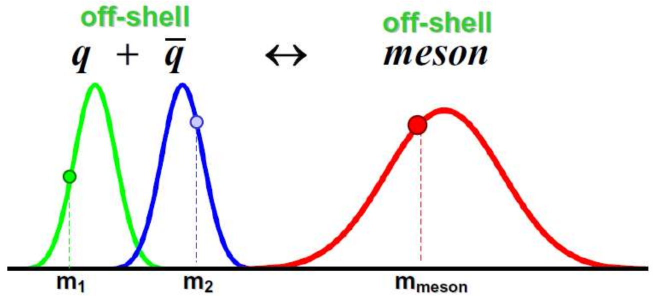

- **Hadronic phase: hadron-hadron interactions – off-shell HSD**

W. Cassing, E. Bratkovskaya, PRC 78 (2008) 034919; NPA831 (2009) 215; W. Cassing, EPJ ST 168 (2009) 3

Partonic energy fraction in central A+A

Time evolution of the partonic energy fraction vs energy

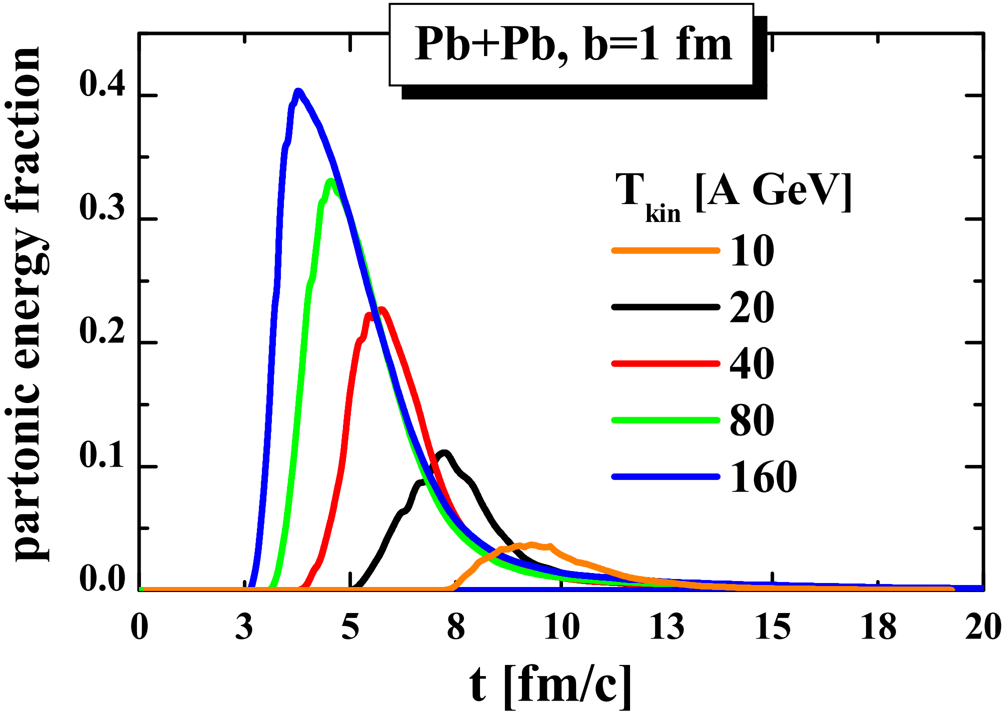

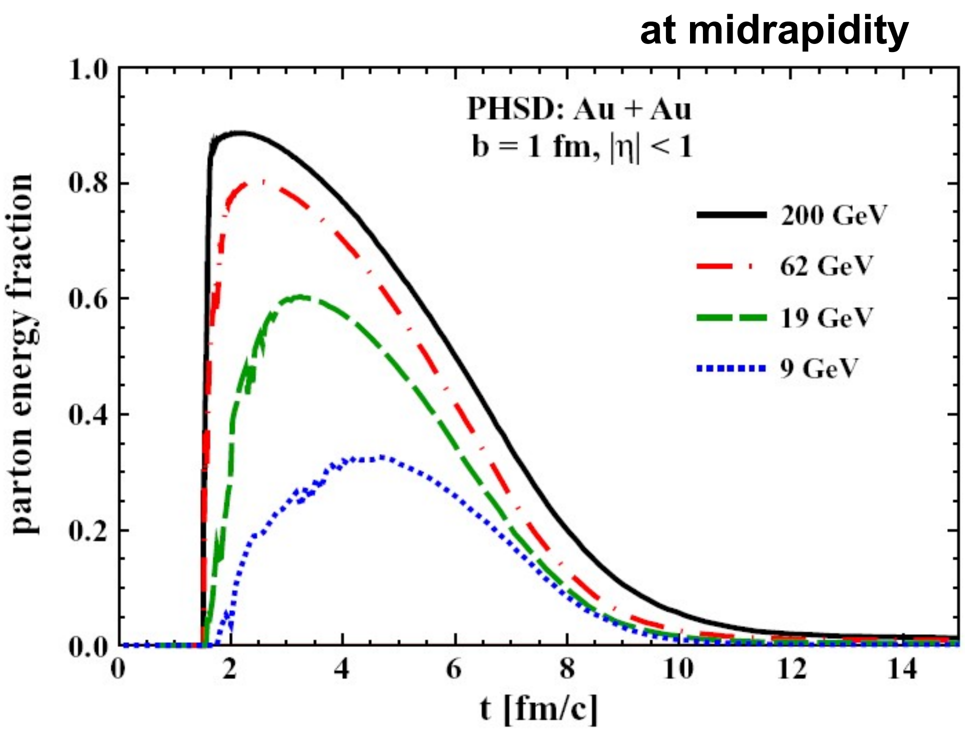

- Strong increase of partonic phase with energy from AGS to RHIC

- SPS: Pb+Pb, 160 A GeV: only about 40% of the converted energy goes to partons; the rest is contained in the large hadronic corona and leading partons
- RHIC: Au+Au, 21.3 A TeV: up to 90% - QGP

W. Cassing & E. Bratkovskaya, NPA 831 (2009) 215
V. Konchakovski et al., Phys. Rev. C 85 (2012) 011902

Transverse mass spectra from SPS to RHIC

Central Pb + Pb at SPS energies | **Central Au+Au at RHIC**

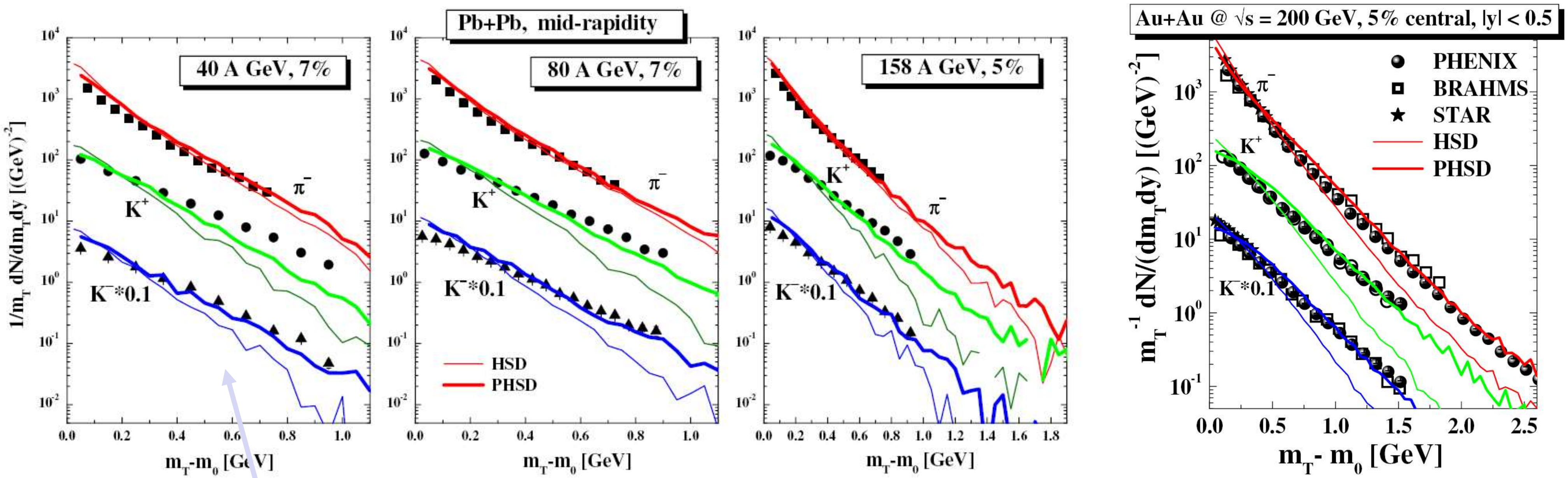

- PHSD gives harder m_T spectra and works better than HSD (wo QGP) at high energies – RHIC, SPS (and top FAIR, NICA)

- however, at low SPS (and low FAIR, NICA) energies the effect of the partonic phase decreases due to the decrease of the partonic fraction

W. Cassing & E. Bratkovskaya, NPA 831 (2009) 215
E. Bratkovskaya, W. Cassing, V. Konchakovski, O. Linnyk, NPA856 (2011) 162

Elliptic flow v_2 vs. collision energy for Au+Au

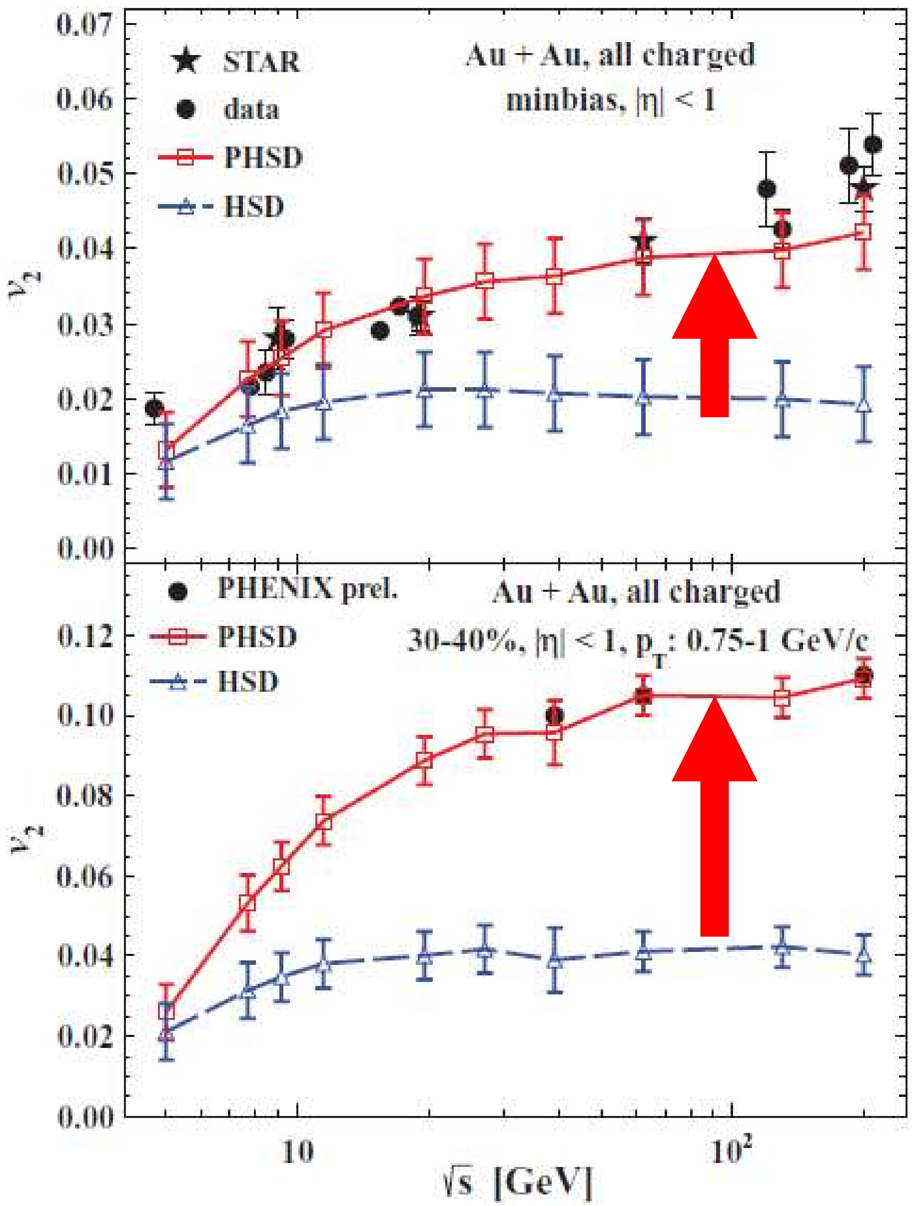

$$\frac{dN}{d\varphi} \propto \left(1 + 2\sum_{n=1}^{+\infty} v_n \cos[n(\varphi - \psi_n)]\right)$$

$$v_n = \langle \cos n(\varphi - \psi_n) \rangle, \quad n = 1,2,3..,$$

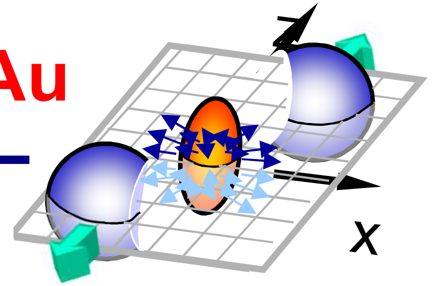

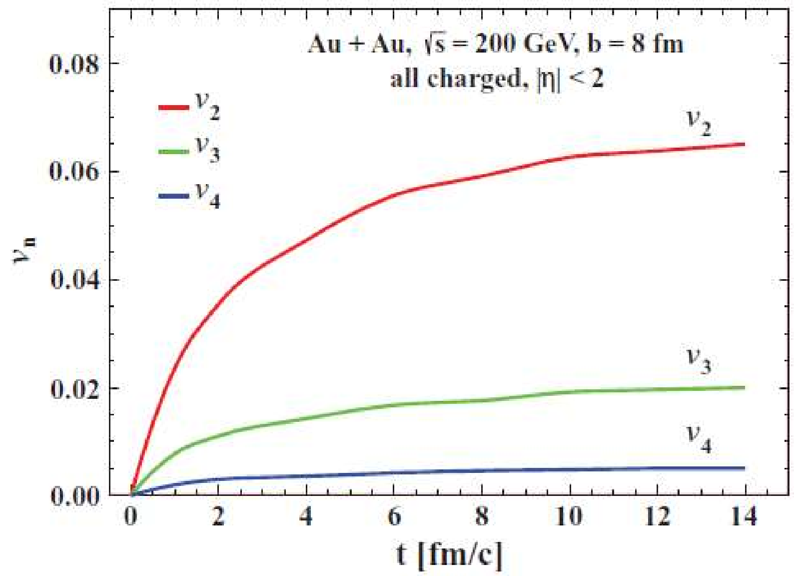

- **v_2 in PHSD is larger than in HSD due to the repulsive scalar mean-field potential $U_s(\rho)$ for partons**
- **v_2 grows with bombarding energy due to the increase of the parton fraction**

V. Konchakovski, E. Bratkovskaya, W. Cassing, V. Toneev, V. Voronyuk, Phys. Rev. C 85 (2012) 011902

Extended DQPM (T, μ_q)

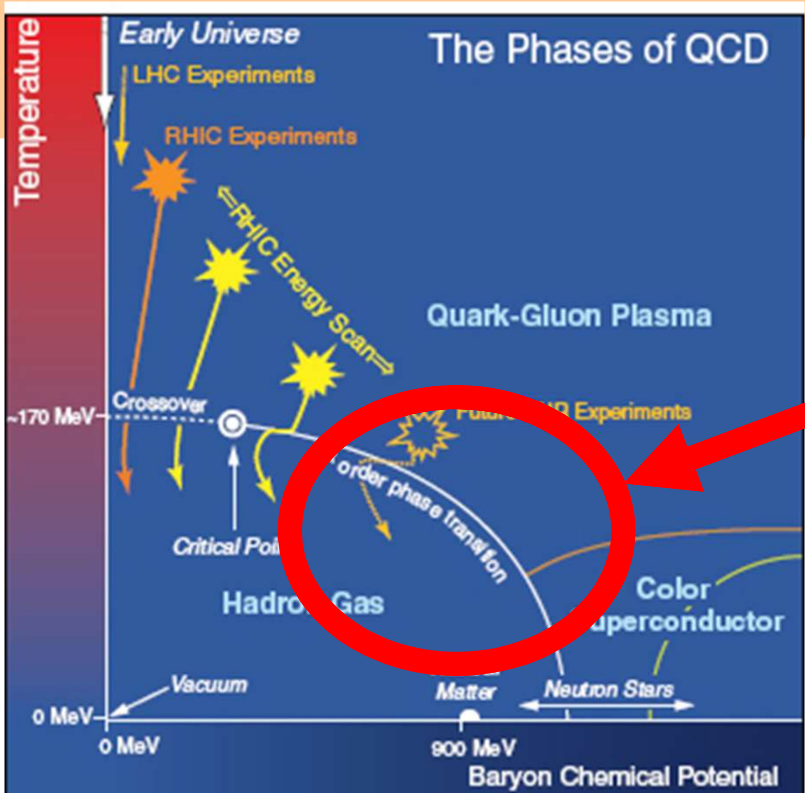

finite μ_q

DQPM at finite (T, μ_q): scaling hypothesis

- **Scaling hypothesis** for the **effective temperature T***
  for $N_f = N_c = 3$

$$\mu_u = \mu_d = \mu_s = \mu_q$$

$$\boxed{T^{*2} = T^2 + \frac{\mu_q^2}{\pi^2}}$$

Jana Guenther

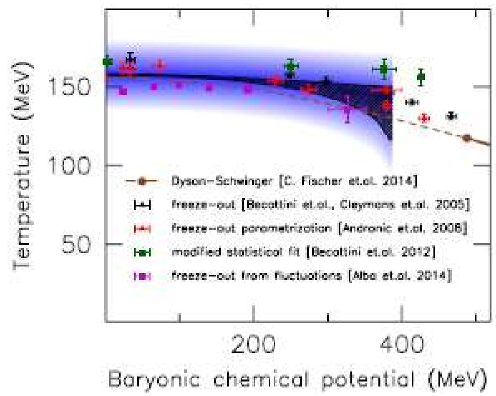

- **Coupling constant:**

$$g(T/T_c(\mu=0)) \longrightarrow g(T^*/T_c(\mu))$$

- **Critical temperature $T_c(\mu_q)$:**

obtained by **requiring a constant energy density ε**
for the system at $T=T_c(\mu_q)$ where ε at $T_c(\mu_q=0)=158$ GeV
is fixed by lQCD at $\mu_q=0$

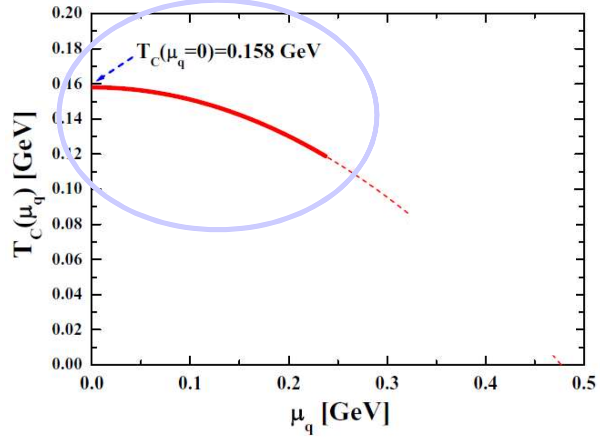

$$\boxed{\frac{T_c(\mu_q)}{T_c(\mu_q=0)} = \sqrt{1-\alpha\,\mu_q^2} \approx 1-\alpha/2\,\mu_q^2 + \cdots}$$

$$\alpha \approx 8.79 \text{ GeV}^{-2}$$

! Consistent with lattice QCD:

lQCD: C. Bonati et al., PRC90 (2014) 114025

$$\frac{T_c(\mu_B)}{T_c} = 1 - \kappa\left(\frac{\mu_B}{T_c}\right)^2 + \cdots$$

lQCD $\kappa = 0.013(2)$ $\longleftrightarrow$ $\kappa_{DQPM} \approx 0.0122$

H. Berrehrah et al, PRC 93 (2016) 044914,
Int.J.Mod.Phys. E25 (2016) 1642003,

From the talk of Christian Schmidt

➡ Curvature of the crossover line is small ….

- $\frac{T_c(\mu_B)}{T_0} = 1 - \kappa_2 \left(\frac{\mu_B}{T_0}\right)^2 - \kappa_4 \left(\frac{\mu_B}{T_0}\right)^4 + \mathcal{O}(\mu_B^6)$
- $\kappa_2 = 0.0123 \pm 0.003$
- $\kappa_4 = 0.000131 \pm 0.0041$

➡ No indication for critical point, limit: $\mu_B^{\mathrm{CEP}} > 400\mathrm{MeV}$

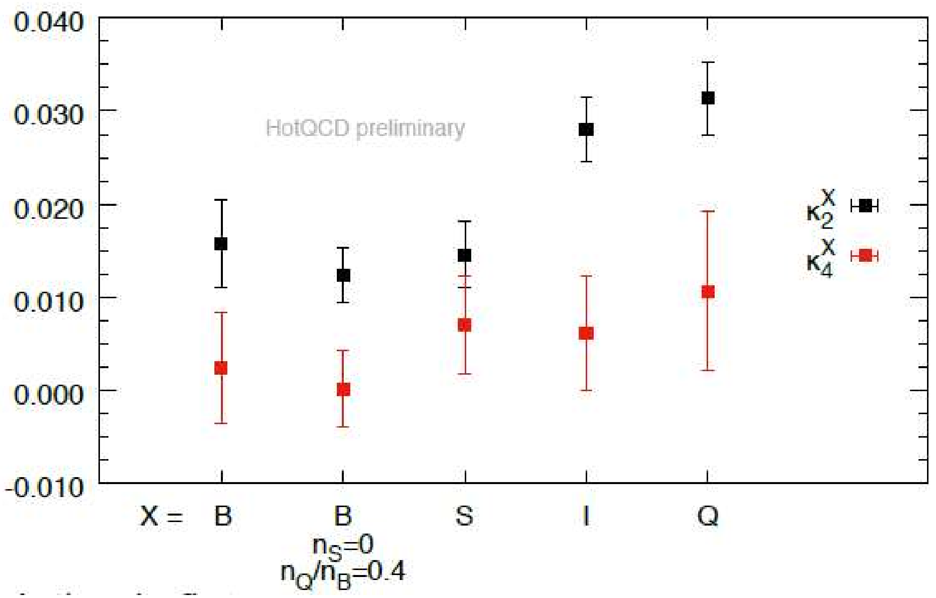

DQPM at finite (T, μ_q): quasiparticle masses and widths

❑ Coupling constant:

$$g^2(T^\star/T_c(\mu_q)) = \frac{48\pi^2}{(11N_c - 2N_f)\ln\left(\lambda^2\left(\frac{T^\star}{T_c(\mu_q)} - \frac{T_s}{T_c(\mu_q)}\right)^2\right)}$$

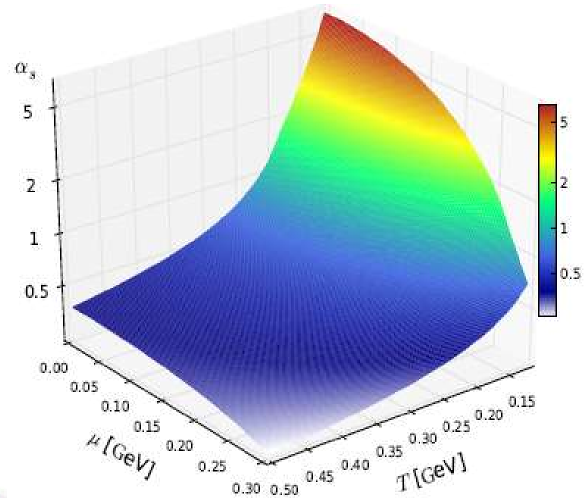

❑ Quark and gluon masses:

$$M_g^2(T^\star,\mu_q) = \frac{g^2(T^\star/T_c(\mu_q))}{6}\left(N_c + \frac{1}{2}N_f\right) T^{\star 2},$$

$$M_q^2(T^\star,\mu_q) = \frac{N_c^2-1}{8N_c} g^2(T^\star/T_c(\mu_q))\, T^{\star 2},$$

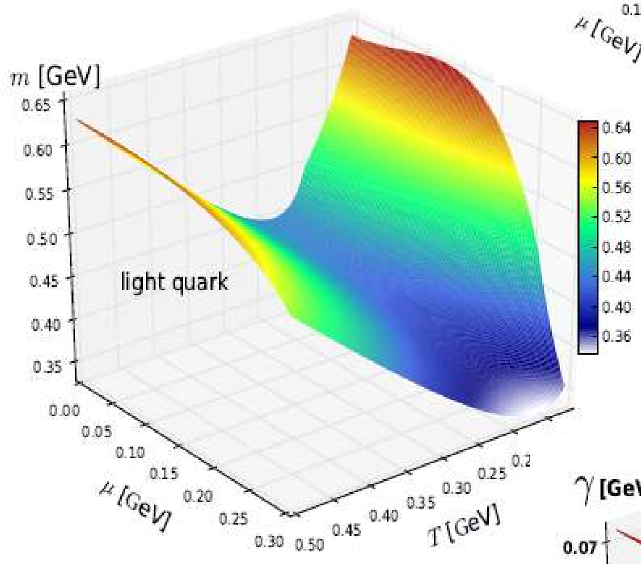

❑ Quark and gluon widths:

$$\gamma_g(T,\mu_q) = \frac{1}{3}N_c \frac{g^2(T^*/T_c(\mu_q))}{8\pi} T \ \ln\left(\frac{2c}{g^2(T^*/T_c(\mu_q))} + 1\right),$$

$$\gamma_q(T,\mu_q) = \frac{1}{3}\frac{N_c^2-1}{2N_c}\frac{g^2(T^*/T_c(\mu_q))}{8\pi} T \ \ln\left(\frac{2c}{g^2(T^*/T_c(\mu_q))} + 1\right).$$

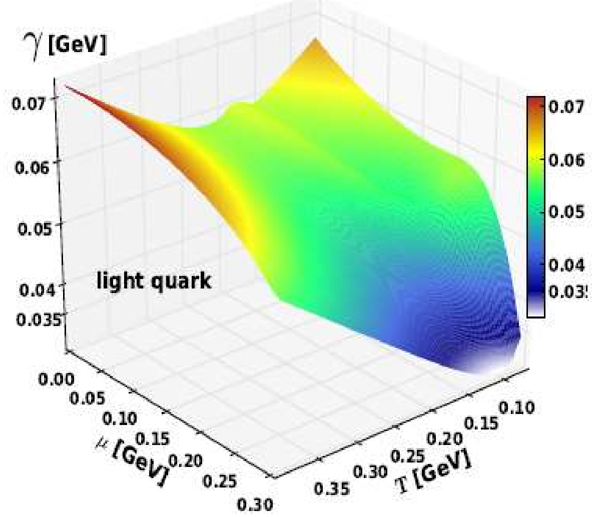

DQPM: thermodynamics at finite (T, μ_q)

- Entropy density, energy density, pressure at finite T

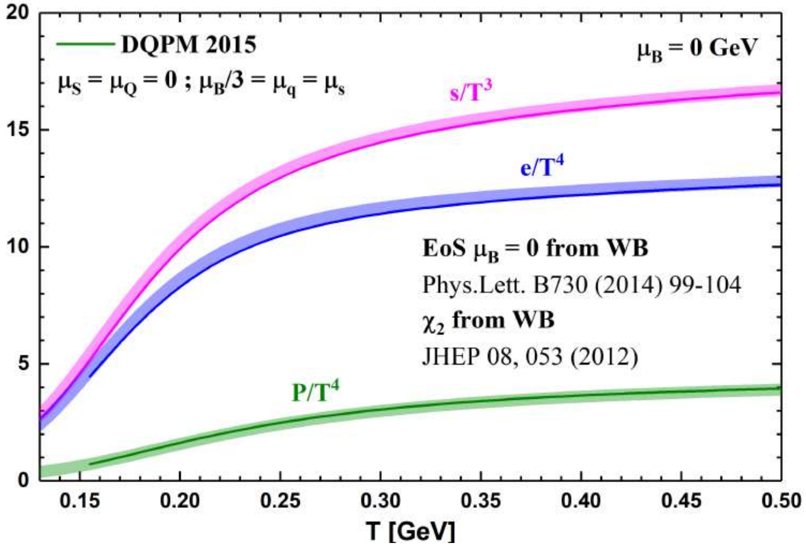

μ_B =0

- Entropy density, energy density, pressure at finite (T, μ_q)

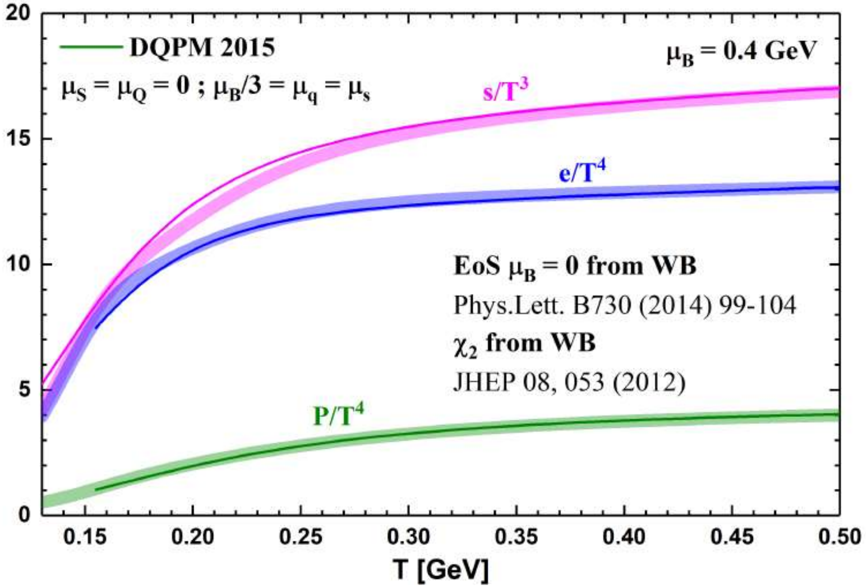

μ_B =400 MeV

H. Berrehrah et al, PRC 93 (2016) 044914,
Int.J.Mod.Phys. E25 (2016) 1642003,

DQPM: q, qbar, g elastic/inelastic scattering (leading order)

q q

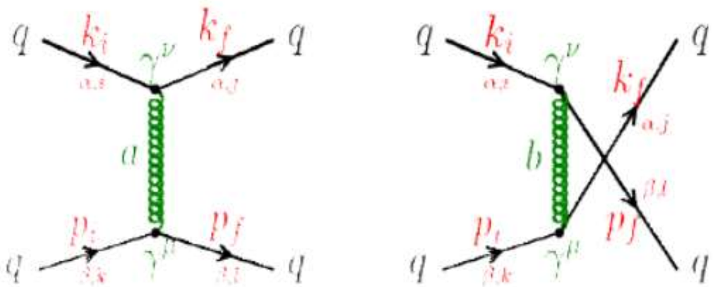

q q̄

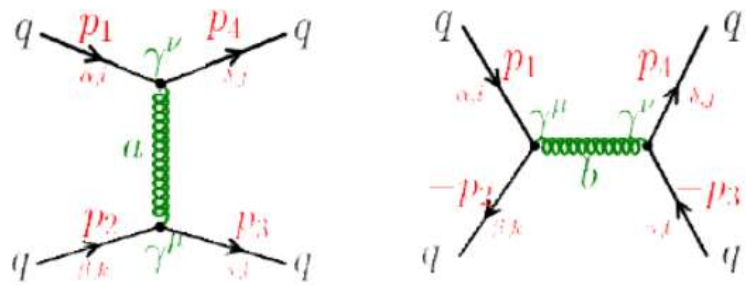

q g

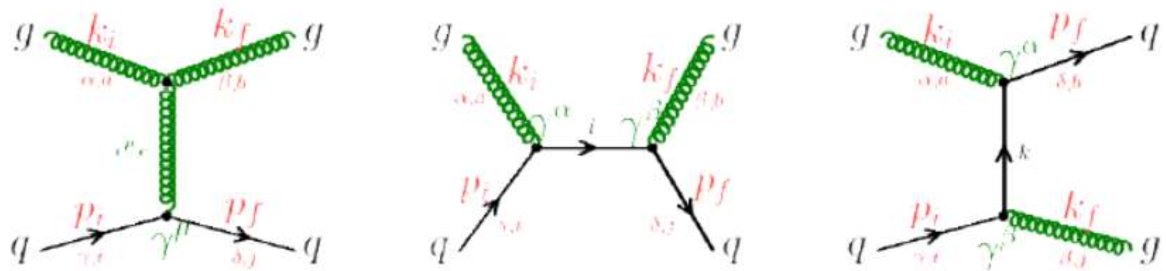

g g

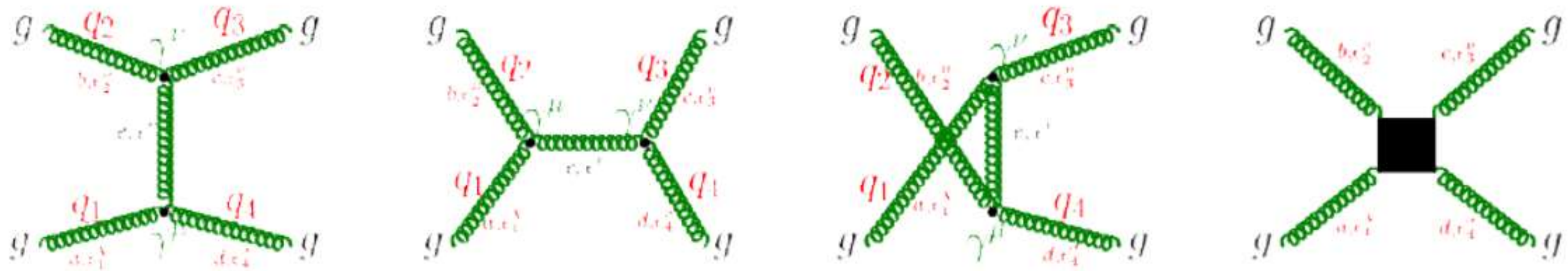

$gg \leftrightarrow q\bar{q}$

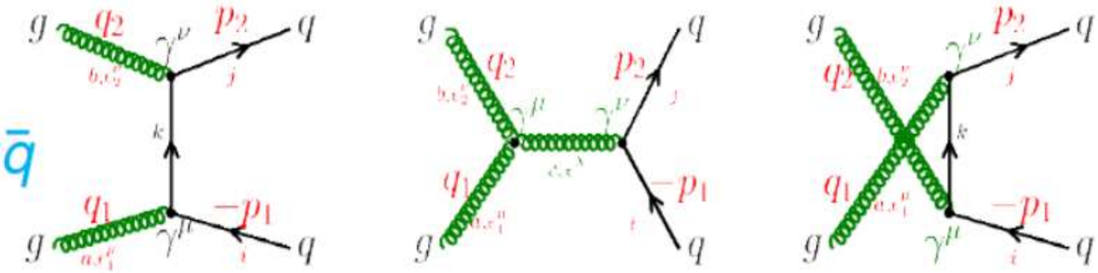

$g \leftrightarrow q\bar{q}$

$g \leftrightarrow gg$

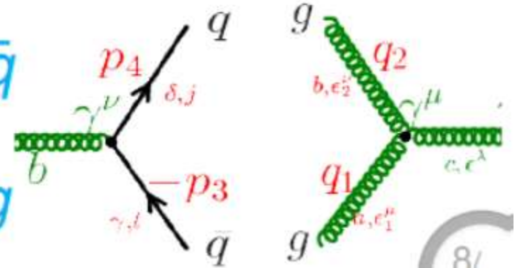

Leading order cross sections in DQPM(T, μ_q)

by Pierre Moreau

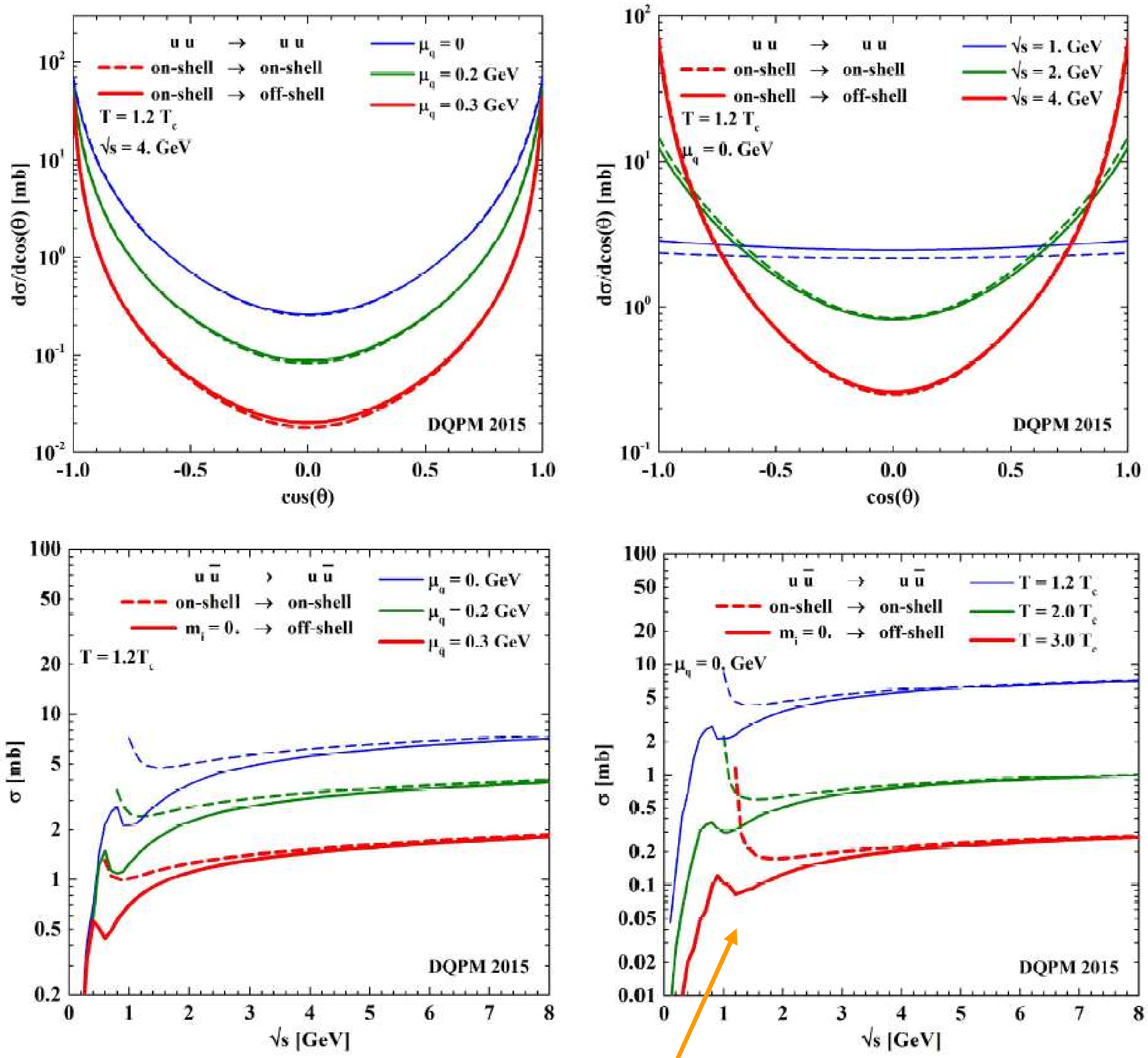

$\sigma(s, m_1, m_2, T, \mu_B)$

- **Off-shell effects of the partons are important!**

H. Berrehrah et al, PRC 93 (2016) 044914, Int.J.Mod.Phys. E25 (2016) 1642003,

Towards a self-consistent DQPM(T, μ_q)

by Pierre Moreau

- **Interaction rates of partons**, ***i =q, qbar, g***

$$\Gamma_i(T,\mu_q) = \frac{1}{n_i^{\rm off}(T,\mu_q)} \int_0^\infty \frac{4\pi\ p_i^2\ dp_i}{(2\pi)^3} \int_0^\infty \frac{d\omega_i}{2\pi}\ 2\omega_i\ \rho_i\ g_i\ f_i\ \Gamma_i(\omega_i, p_i, T, \mu_q).$$

$$\Gamma_i(E_i, p_i, T, \mu_q) = \frac{1}{2E_i} \sum_{j=q,\bar{q},g} \int \frac{d^4p_j}{(2\pi)^4}\ g_j\ f_j\ \theta(\omega_j)\ \rho_j \int \frac{d^4p_3}{(2\pi)^4}\ \theta(\omega_3)\ \rho_3 \int \frac{d^4p_4}{(2\pi)^4}\ \theta(\omega_4)\ \rho_4$$

$$(1 \pm f_3)(1 \pm f_4)\ |\bar{\mathcal{M}}|^2(p_i, p_j, p_3, p_4)\ (2\pi)^4 \delta^{(4)}(p_i + p_j - p_3 - p_4), \qquad \text{(B.34)}$$

$$= \sum_{j=q,\bar{q},g} \int \frac{d^4p_j}{(2\pi)^4}\ g_j\ f_j\ \theta(\omega_j)\ \rho_j\ v_{\rm rel} \int d\sigma_{ij\to 34}^{\rm off} (1 \pm f_3)(1 \pm f_4), \qquad \text{(B.35)}$$

Example: gluons

$$n_i^{\rm off}(T,\mu_q) = \int_0^\infty \frac{4\pi\ p_i^2\ dp_i}{(2\pi)^3} \int_0^\infty \frac{d\omega_i}{2\pi}\ 2\omega_i\ \rho_i\ g_i\ f_i$$

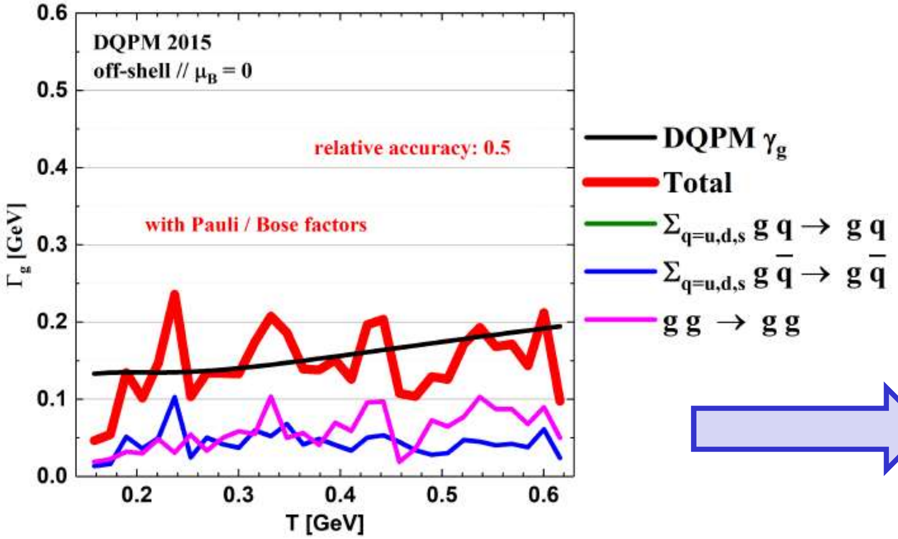

the initial width is recovered !

→ **DQPM is already self-consistent!**

DQPM(T, μ_q): n_B , χ_q

❑ Baryon number density n_B , susceptibilities χ_q at finite (T, μ)

$$\chi_q(T) = \left.\frac{\partial n_q}{\partial \mu_q}\right|_{\mu_q=0}; \quad \chi_q(T,\mu_q) = \frac{1}{9}\frac{\partial n_B}{\partial \mu_B}. \qquad \chi_2(T) = \frac{1}{9}\frac{1}{T^2}\left.\frac{\partial n_q(T,\mu_q)}{\partial \mu_q}\right|_{\mu_q=0} = \frac{1}{9}\frac{\chi_q(T)}{T^2}$$

for 3 flavours with $\mu_u = \mu_d = \mu_s = \mu_q$

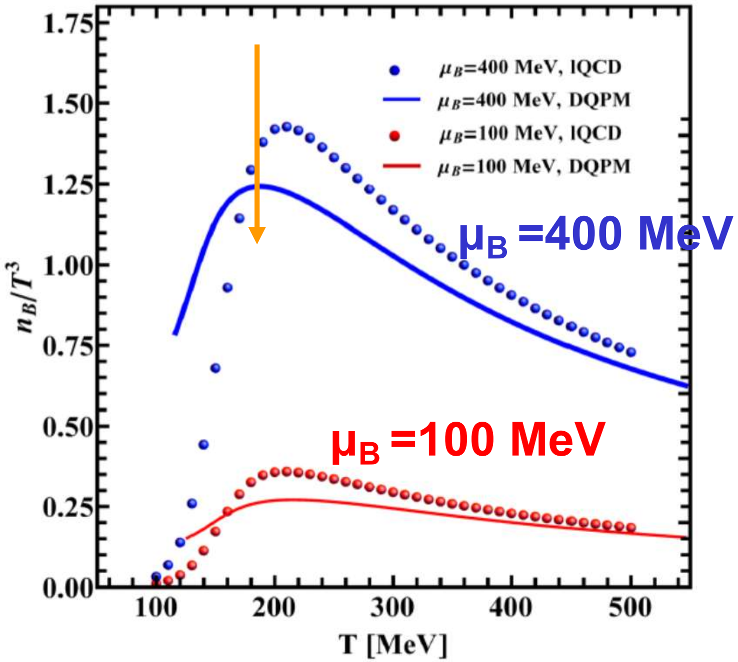

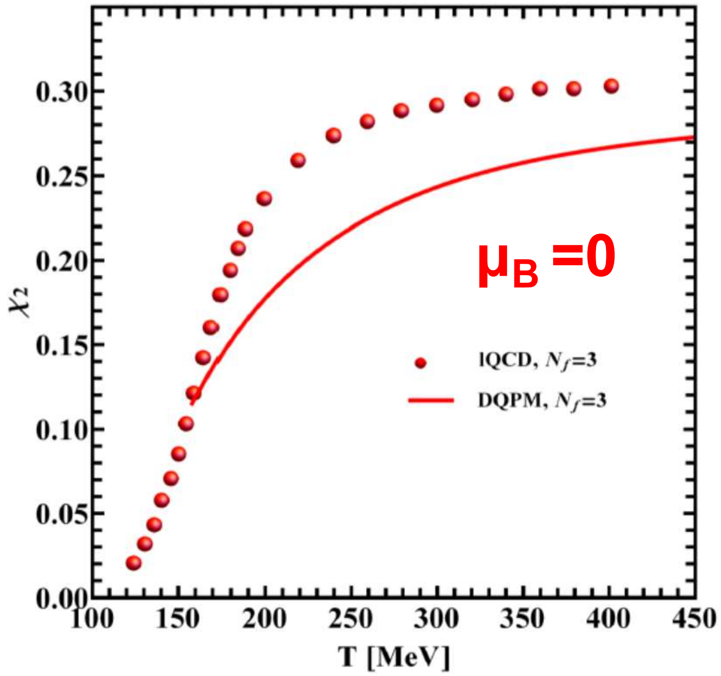

- ○ **Comparison to lQCD : n_B, χ_q from DQPM is lower then lQCD data**
- ○ **Quarks / gluons from DQPM are too heavy?**

H. Berrehrah et al, PRC 93 (2016) 044914, Int.J.Mod.Phys. E25 (2016) 1642003,

DQPM* (T, μ_q,p)

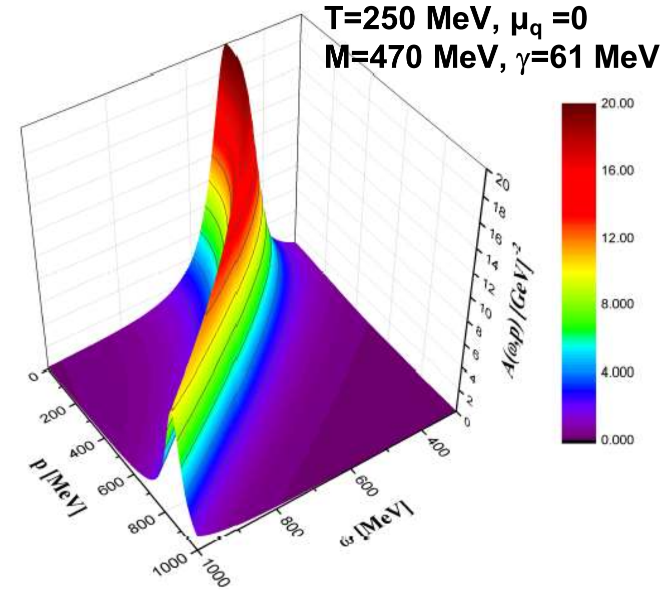

DQPM* at finite (T, μ_q,p): quasiparticle masses and widths

- **Momentum-dependent Lorentzian spectral function :**

H. Berrehrah et al, PRC 93 (2016) 044914, arXiv:1512.06909; Int.J.Mod.Phys. E25 (2016) 1642003, arXiv:1605.02371

$$\rho_i(\omega,\boldsymbol{p}) = \frac{\gamma_i(\boldsymbol{p})}{\tilde{E}_i(\boldsymbol{p})}\left(\frac{1}{(\omega-\tilde{E}_i(\boldsymbol{p}))^2+\gamma_i^2(\boldsymbol{p})} - \frac{1}{(\omega+\tilde{E}_i(\boldsymbol{p}))^2+\gamma_i^2(\boldsymbol{p})}\right)$$

$$\tilde{E}_i^2(\boldsymbol{p}) = \boldsymbol{p}^2 + M_i^2(\boldsymbol{p}) - \gamma_i^2(\boldsymbol{p}) \text{ for } i \in [g,q,\bar{q}].$$

- ***p* dependence of $m_{q,\,g}$ inspired by Dyson-Schwinger results**

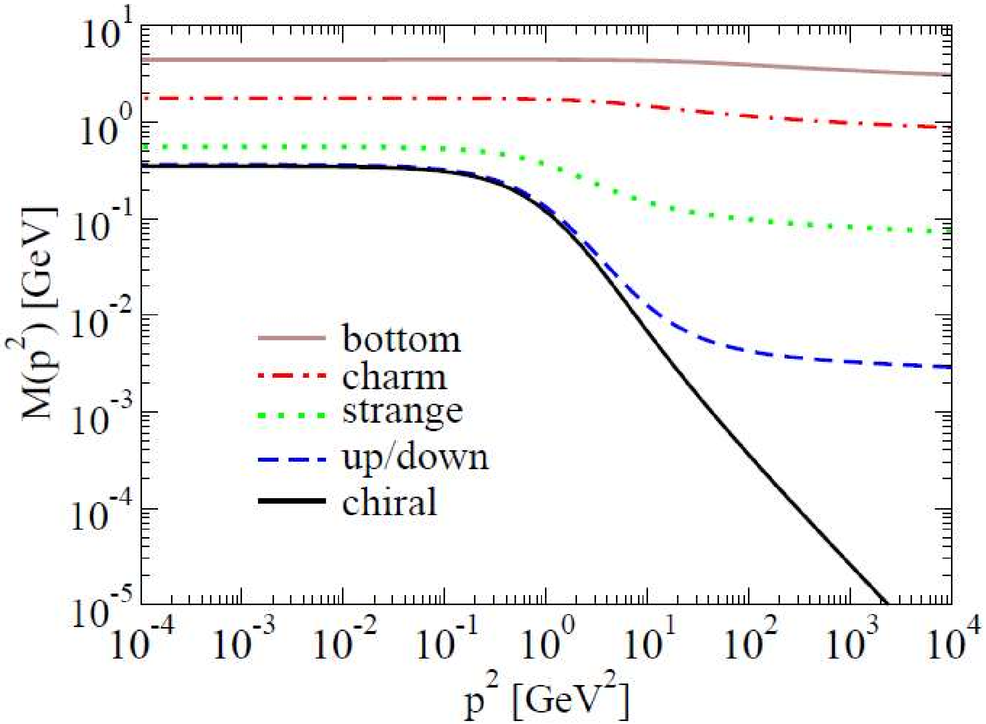

Ch.S. Fischer J. Phys. G: Nucl. Part. Phys. 32 (2006) R253–R291

Euclidean-4-momentum squared

$p^2 = \omega^2 + \mathbf{p}^2$

DQPM* at finite (T, μ_q,p): quasiparticle masses and widths

H. Berrehrah et al, PRC 93 (2016) 044914, arXiv:1512.06909;
Int.J.Mod.Phys. E25 (2016) 1642003, arXiv:1605.02371

- **Quark and gluon masses:**

$$M_g(T,\mu_q,p) = \left(\frac{3}{2}\right)\left[\frac{g^2(T^\star/T_c(\mu_q))}{6}\left[\left(N_c+\frac{N_f}{2}\right)T^2+\frac{N_c}{2}\sum_q\frac{\mu_q^2}{\pi^2}\right]\right]^{1/2}\times h(\Lambda_g,p)+m_{\chi g}\,,$$

$$M_{q,\bar{q}}(T,\mu_q,p) = \left[\frac{N_c^2-1}{8N_c}\,g^2(T^\star/T_c(\mu_q))\left[T^2+\frac{\mu_q^2}{\pi^2}\right]\right]^{1/2}\times h(\Lambda_q,p)+m_{\chi q}\,,$$

$$\boxed{h(\Lambda,p) = \left[\frac{1}{1+\Lambda(T_c(\mu_q)/T^\star)p^2}\right]^{1/2}}$$

- **Quark and gluon widths:**

$$\Lambda_g(T_c(\mu_q)/T^\star) = 5\ \ (T_c(\mu_q)/T^\star)^2\ \mathrm{GeV}^{-2}$$

$$\Lambda_q(T_c(\mu_q)/T^\star) = 12\ \ (T_c(\mu_q)/T^\star)^2\ \mathrm{GeV}^{-2}$$

$$\gamma_g(T,\mu_q,p) = N_c\,\frac{g^2(T^\star/T_c(\mu_q))}{8\pi}\,T\,\ln\left(\frac{2c}{g^2(T^\star/T_c(\mu_q))}+1.1\right)^{3/4}\times h(\Lambda_g,p)\,,$$

$$\gamma_{q,\bar{q}}(T,\mu_q,p) = \frac{N_c^2-1}{2N_c}\,\frac{g^2(T^\star/T_c(\mu_q))}{8\pi}\,T\ln\left(\frac{2c}{g^2(T^\star/T_c(\mu_q))}+1.1\right)^{3/4}\times h(\Lambda_q,p)$$

The final quark masses for the limits $p\to 0$ and $T=0$ or for $p\to\infty$

$m_{\chi q}=0.003$ GeV for u, d quarks and $m_{\chi q}=0.06$ GeV for s quarks

The gluon condensate: $m_{\chi g}=0.5$ GeV

- **Effective temperature T* for N_f = N_c = 3 (as in extended DQPM)**

$$\boxed{T^{*2} = T^2+\frac{\mu_q^2}{\pi^2}}$$

DQPM* at finite (T, μ_q,p): quasiparticle masses and widths

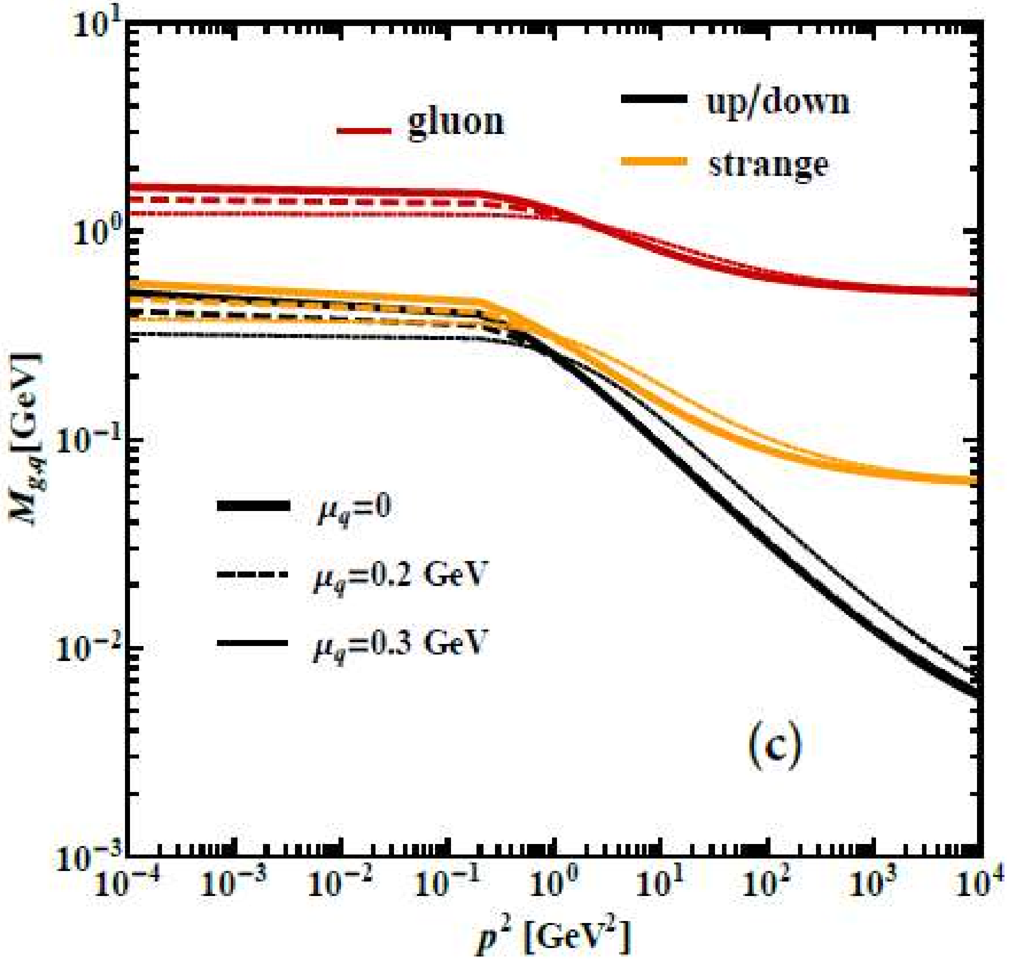

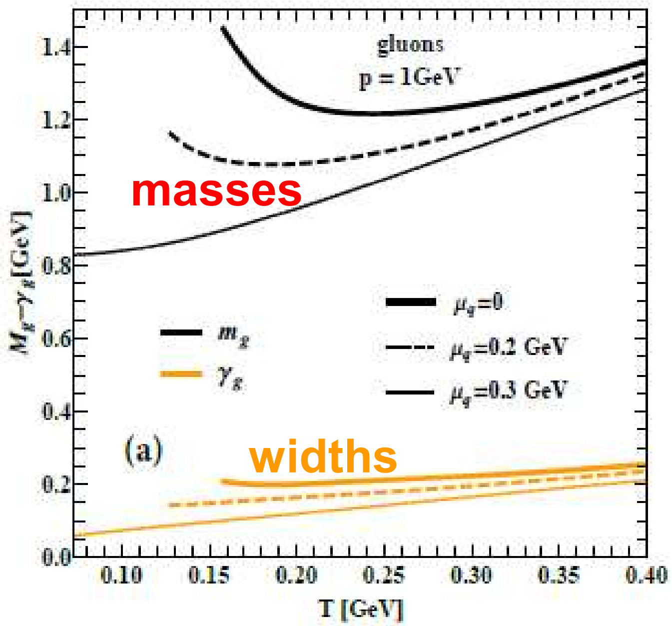

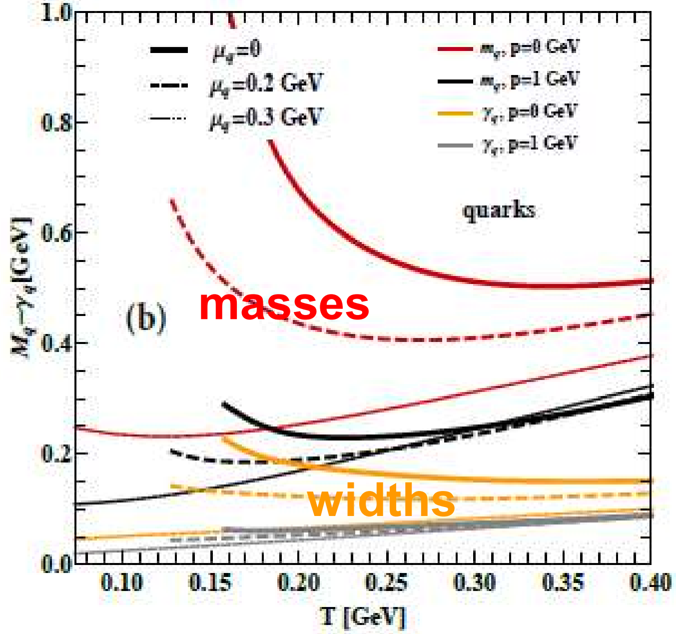

- **With increasing *p* momenta:** $M_{q,g}$ and $\gamma_{q,g}$ **decrease** at T, μ_q
- $\mu_q = 0$ → finite μ_q: decrease of $M_{q,g}$ and $\gamma_{q,g}$

H. Berrehrah et al, PRC 93 (2016) 044914, arXiv:1512.06909; Int.J.Mod.Phys. E25 (2016) 1642003, arXiv:1605.02371

QGP Thermodynamics from DQPM* (T, μ_q,p)

EoS from DQPM* at finite (T, μ_B)

Nf=3; lQCD, Sz. Borsanyi et al., JHEP08(2012)053

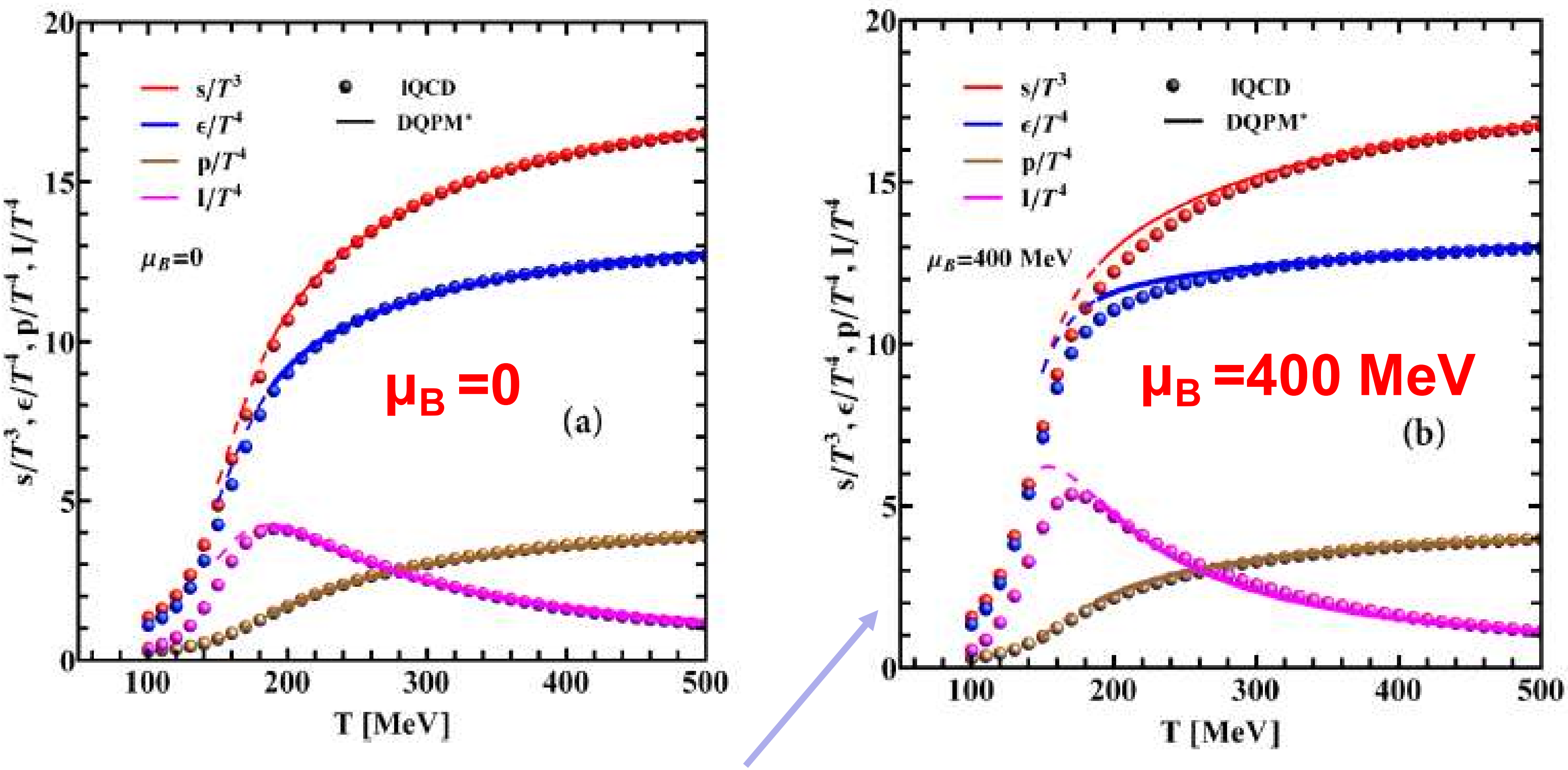

- High T (T>1.2 $T_c(\mu)$): very good agreement with the lattice data
- Low T (T<1.2 $T_c(\mu)$): some deviations → additional hadronic d.o.f. in the crossover region ?

H. Berrehrah et al, PRC 93 (2016) 044914, arXiv:1512.06909;
Int.J.Mod.Phys. E25 (2016) 1642003, arXiv:1605.02371

QGP Thermodynamics from DQPM* (T, μ_q,p)

❑ n_B , χ_q at finite (T, μ_B)

$$\chi_q(T) = \frac{\partial n_q}{\partial \mu_q}\bigg|_{\mu_q=0}; \qquad \chi_q(T,\mu_q) = \frac{1}{9}\frac{\partial n_B}{\partial \mu_B}. \qquad \chi_2(T) = \frac{1}{9}\frac{1}{T^2}\frac{\partial n_q(T,\mu_q)}{\partial \mu_q}\bigg|_{\mu_q=0} = \frac{1}{9}\frac{\chi_q(T)}{T^2}$$

for 3 flavours with $\mu_u = \mu_d = \mu_s = \mu_q$

DQPM

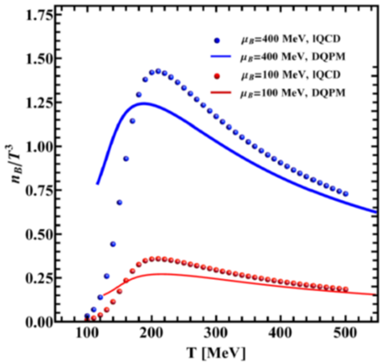

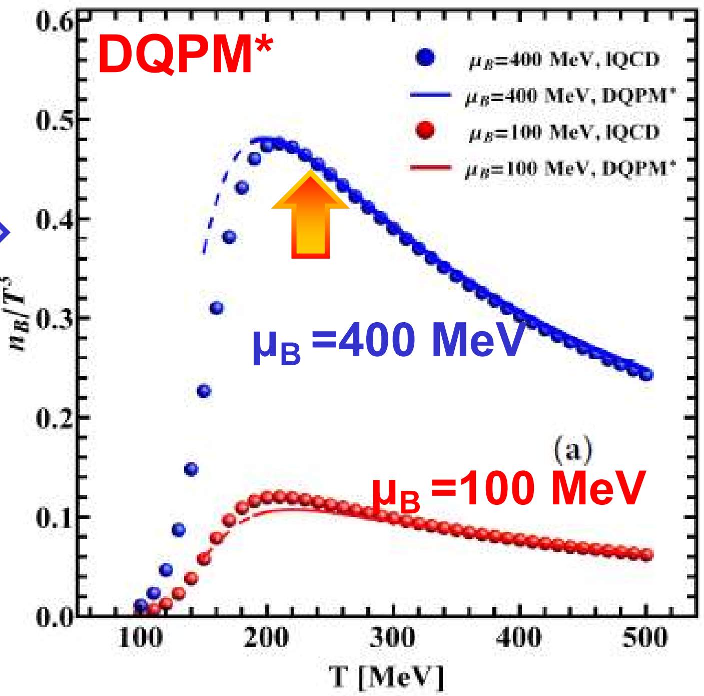

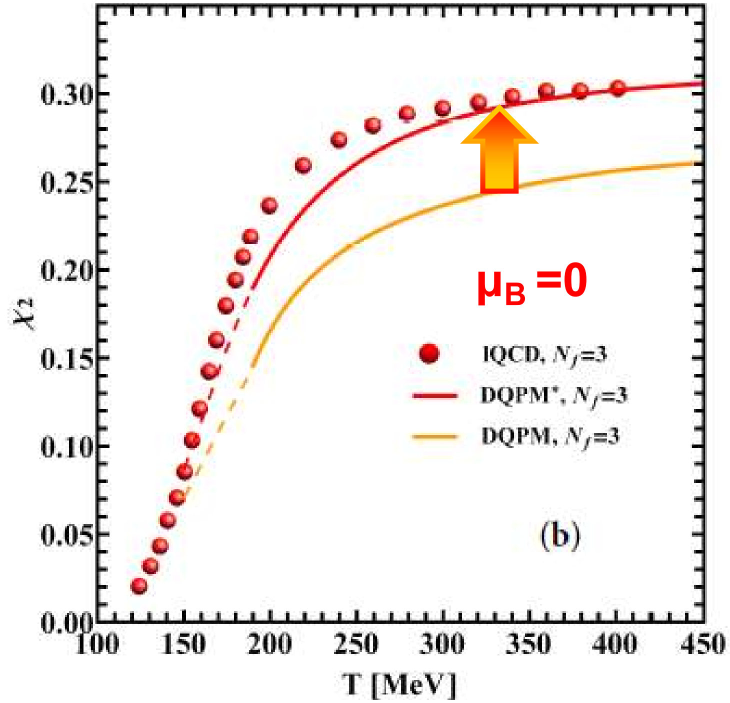

- DQPM* describes n_B, quark susceptibility and entropy/pressure…
- p dependence of partonic masses allows DQPM* to meet lQCD

H. Berrehrah et al, PRC 93 (2016) 044914, arXiv:1512.06909;
Int.J.Mod.Phys. E25 (2016) 1642003, arXiv:1605.02371

Thermodynamical consistency of DQPM* (T, μ_q,p)

- DQPM* at finite temperature and chemical potential (T, μ_B) determined by **thermodynamic consistency:**

Maxwell relation: $$\left.\frac{\partial s}{\partial \mu_B}\right|_T = \left.\frac{\partial n_B}{\partial T}\right|_{\mu_B}$$

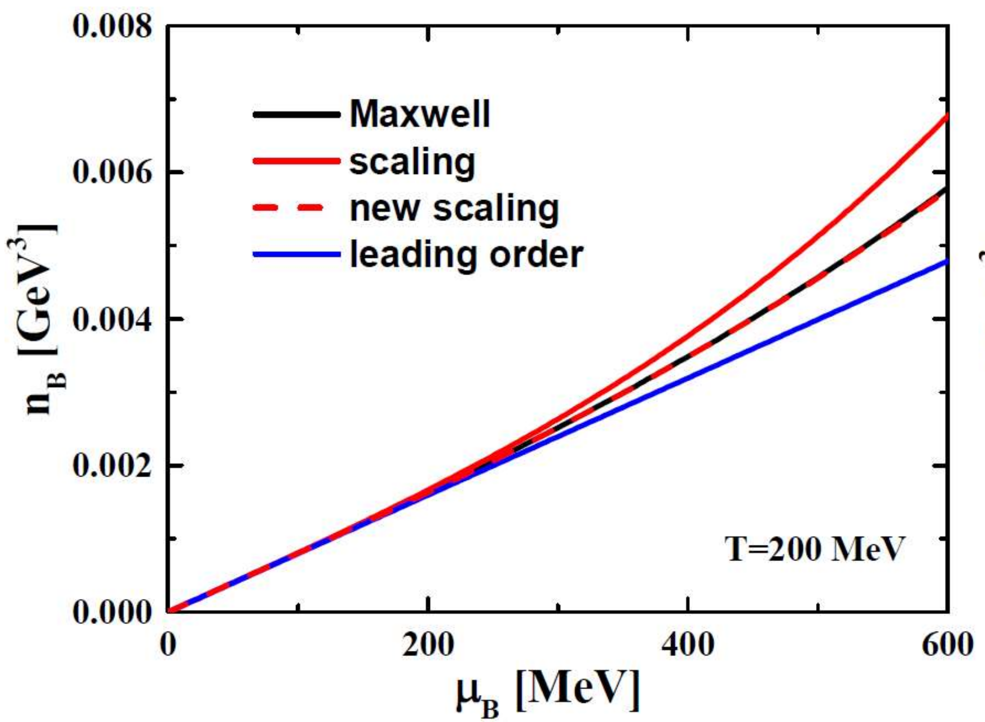

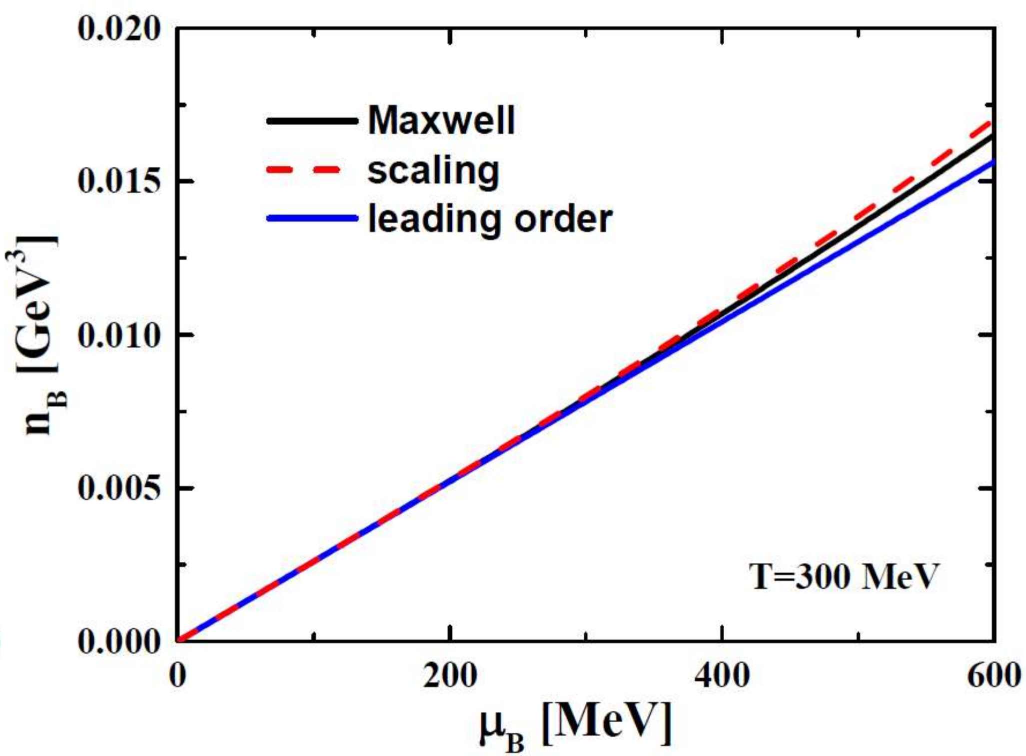

- **Leading order in $n_B = \chi_q * \mu_B$**
- **Scaling relation :** $\frac{T_c(\mu_q)}{T_c(\mu_q=0)} = \sqrt{1-\alpha\,\mu_q^2} \approx 1-\alpha/2\,\mu_q^2 + \cdots$
- **New Scaling: α is determined by Maxwell relation**

from T. Steinert
PhD Thesis (Giessen, 2018)
http://geb.uni-giessen.de/geb/volltexte/2018/13621/

DQPM *(T, μ_q, p) :
transport properties at finite (T, μ_q)

(based on relaxation time approximation - RTA)

DQPM*: transport properties at finite (T, μ_q) : η/s

Shear viscosity η/s at finite T

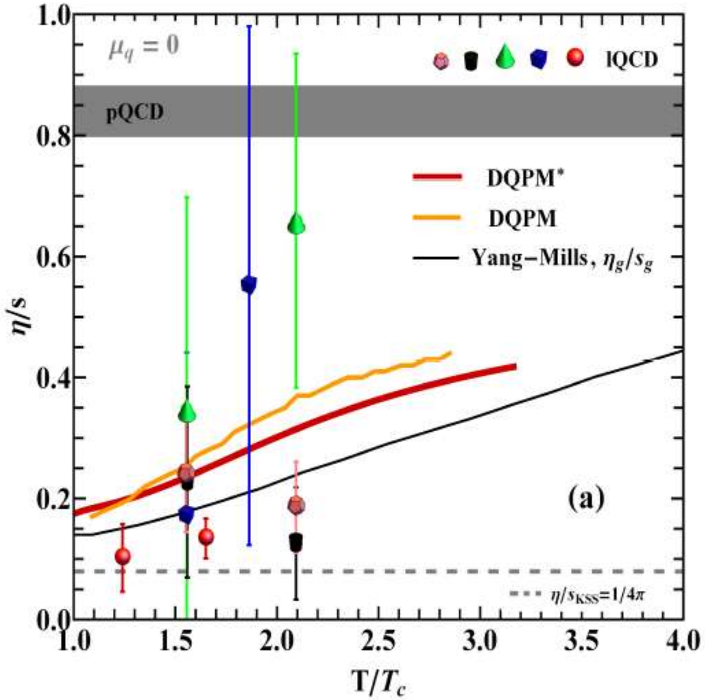

Shear viscosity η/s at finite (T, μ_q)

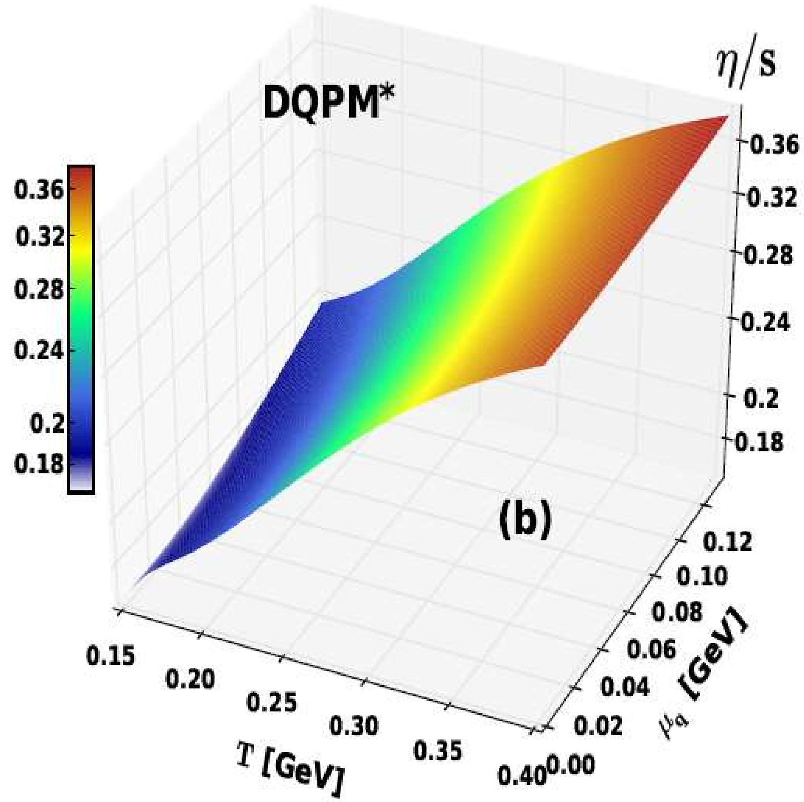

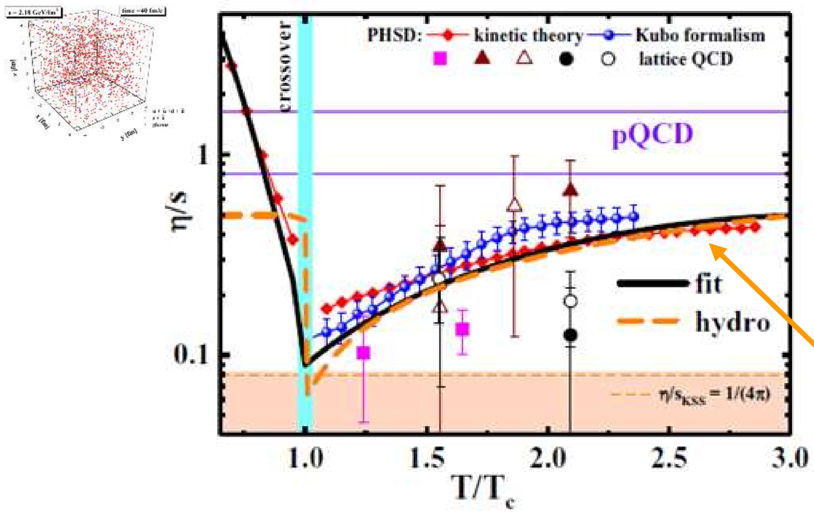

η/s: μ_q=0 ➔ finite μ_q:
smooth increase as a function of (T, μ_q)

H. Berrehrah et al, PRC 93 (2016) 044914, arXiv:1512.06909; Int.J.Mod.Phys. E25 (2016) 1642003, arXiv:1605.02371

PHSD in a box: V. Ozvenchuk et al., PRC 87 (2013) 064903
Hydro: Bayesian analysis, S. Bass et al., 1704.07671

DQPM*: transport properties at finite (T, μ_q): σ_e/T

Electric conductivity σ_e/T at finite T

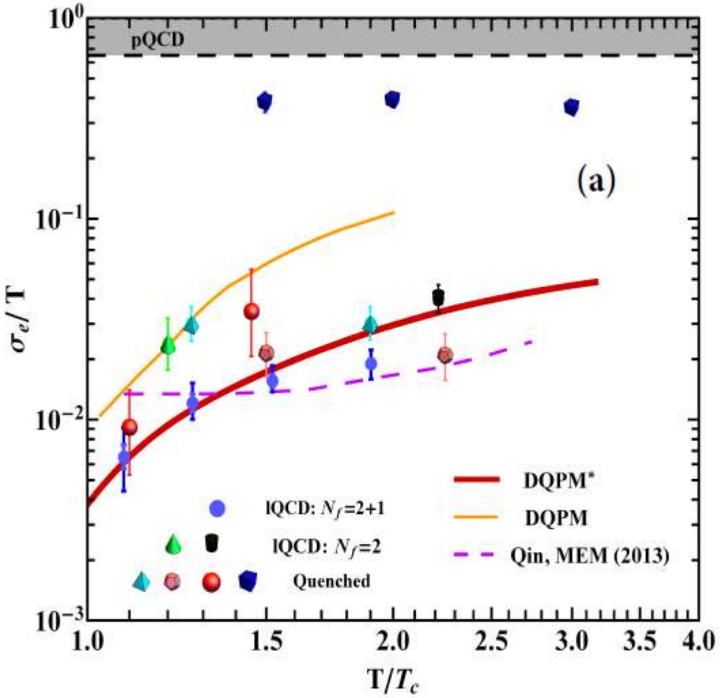

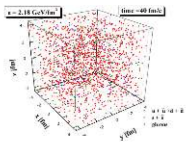

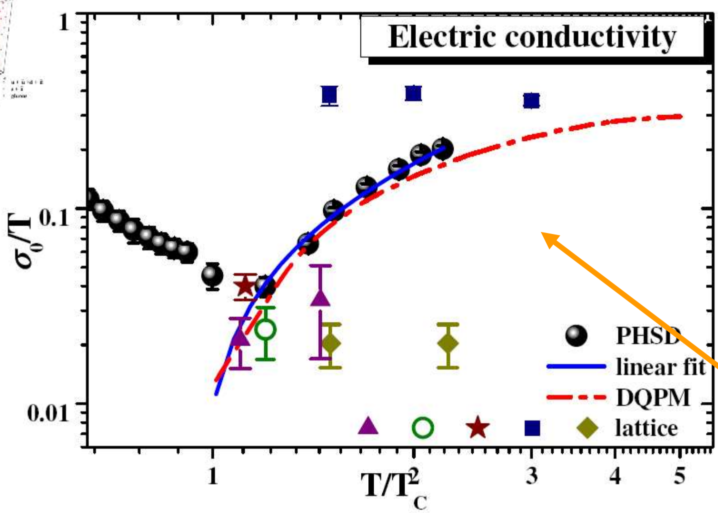

Electric conductivity σ_e/T at finite (T, μ_q)

$$\sigma_e(T,\mu_q) = \sum_{f,\bar{f}}^{u,d,s} \frac{e_f^2\, n_f^{\rm off}(T,\mu_q)}{\bar{\omega}_f(T,\mu_q)\,\bar{\gamma}_f(T,\mu_q)}$$

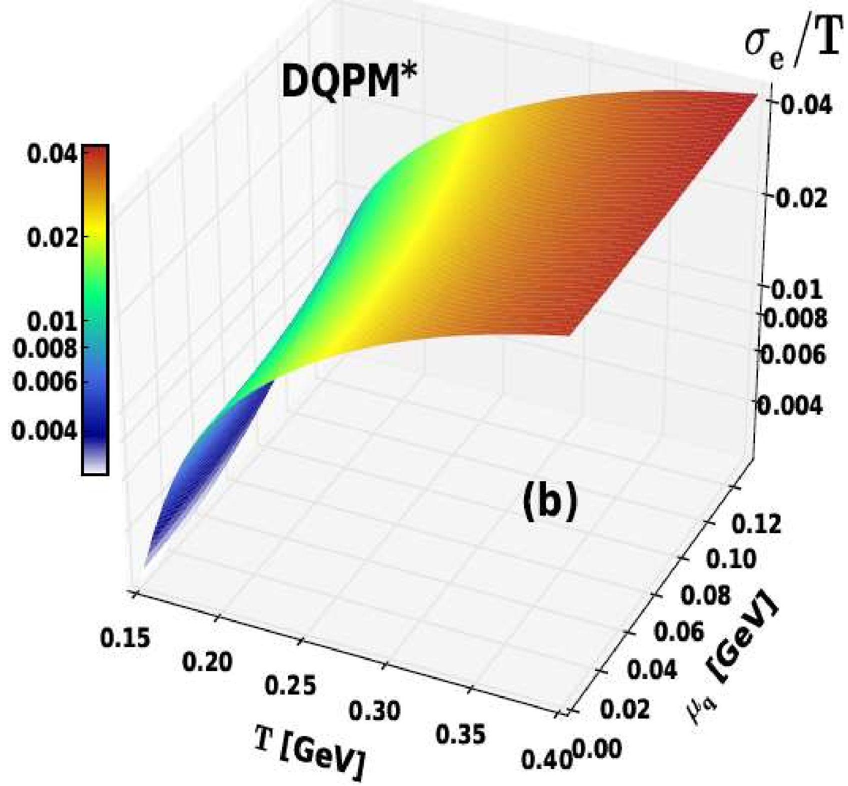

σ_e/T : μ_q=0 ➔ finite μ_q:
smooth variation as a function of (T, μ_q)

H. Berrehrah et al, PRC 93 (2016) 044914, arXiv:1512.06909;
Int.J.Mod.Phys. E25 (2016) 1642003, arXiv:1605.02371

PHSD in a box: V. Ozvenchuk et al., PRC 87 (2013) 064903

Summary: DQPM, DQPM* at finite (T, μ_q)

- Extension of the DQPM to finite μ_q using a scaling hypothesis for the effective temperature T*
- Check of self-consistency of the DQPM
- DQPM is consistent with Maxwell relations
- μ_q=0 ➔ finite μ_q:
  - variations in the QGP transport coefficients
  - smooth dependence on (T, μ_q)
  - η/s, ζ/s, σ_e/T, D_s show minima around T_C at μ_q=0 and finite μ_q
- additional p dependence of masses allows DQPM* to meet lQCD: DQPM* describes n_B, quark susceptibility and entropy/pressure…

Work in progress:

Implementation into PHSD: from DQPM(T) ➔ DQPM(T, μ_q)

Traces of the QGP **at finite μ_q** in observables in high energy heavy-ion collisions

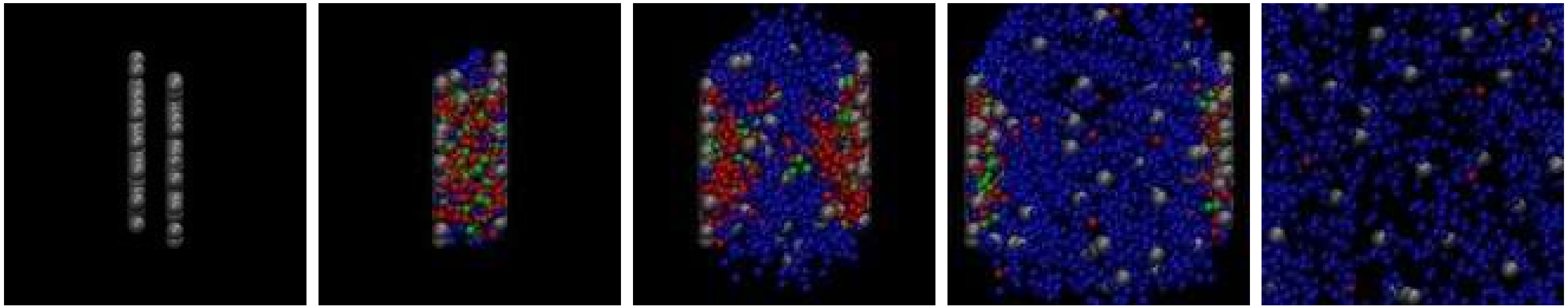

PHSD with DQPM(T, μ_q)

Extraction of T and μ_q from PHSD:

by Pierre Moreau

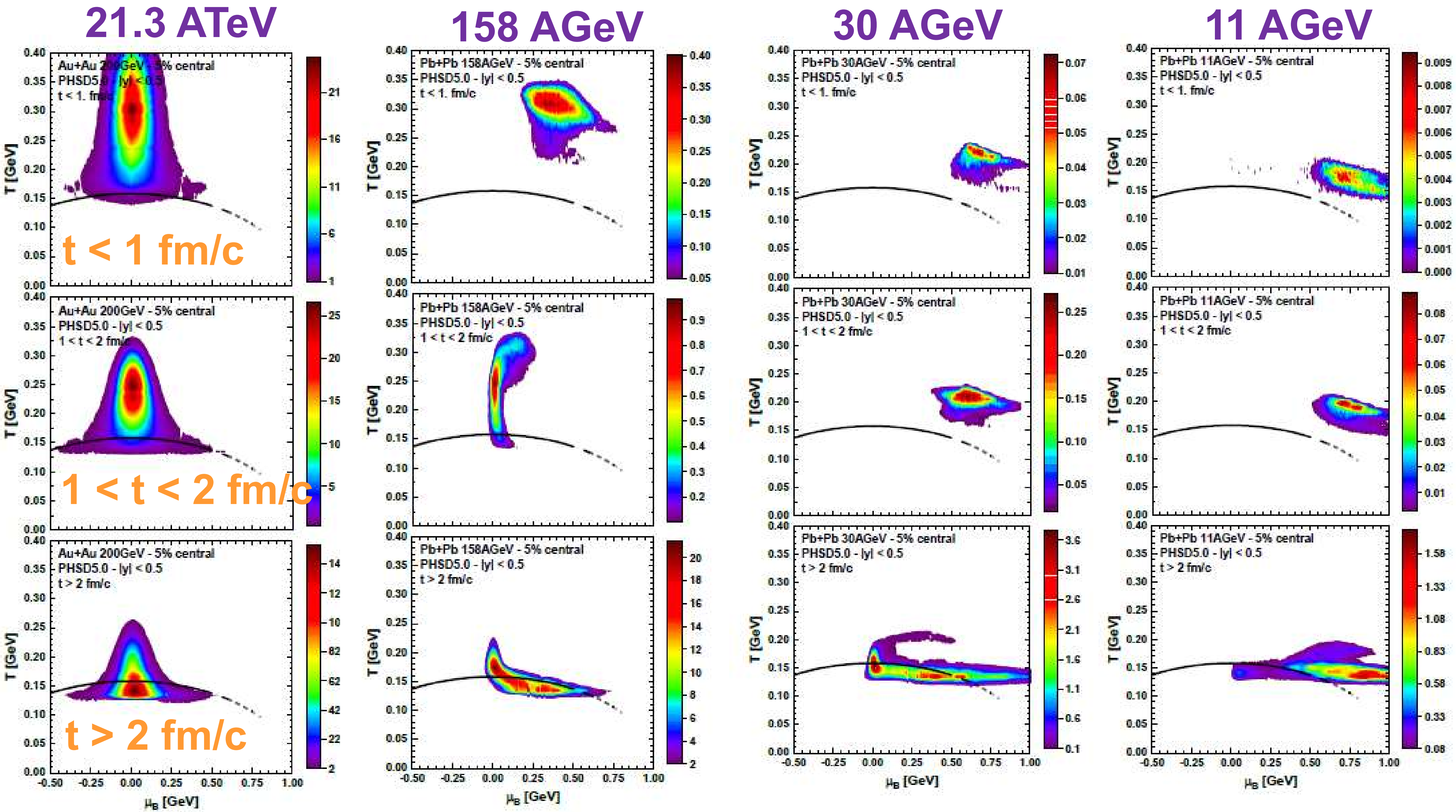

* The scale corresponds to the number of cells (with ε >0.1 GeV/fm^3) per PHSD event counted in the considered bin in T - μ_B

PHSD with DQPM(T, μ_q)

by Pierre Moreau, Olga Soloveva

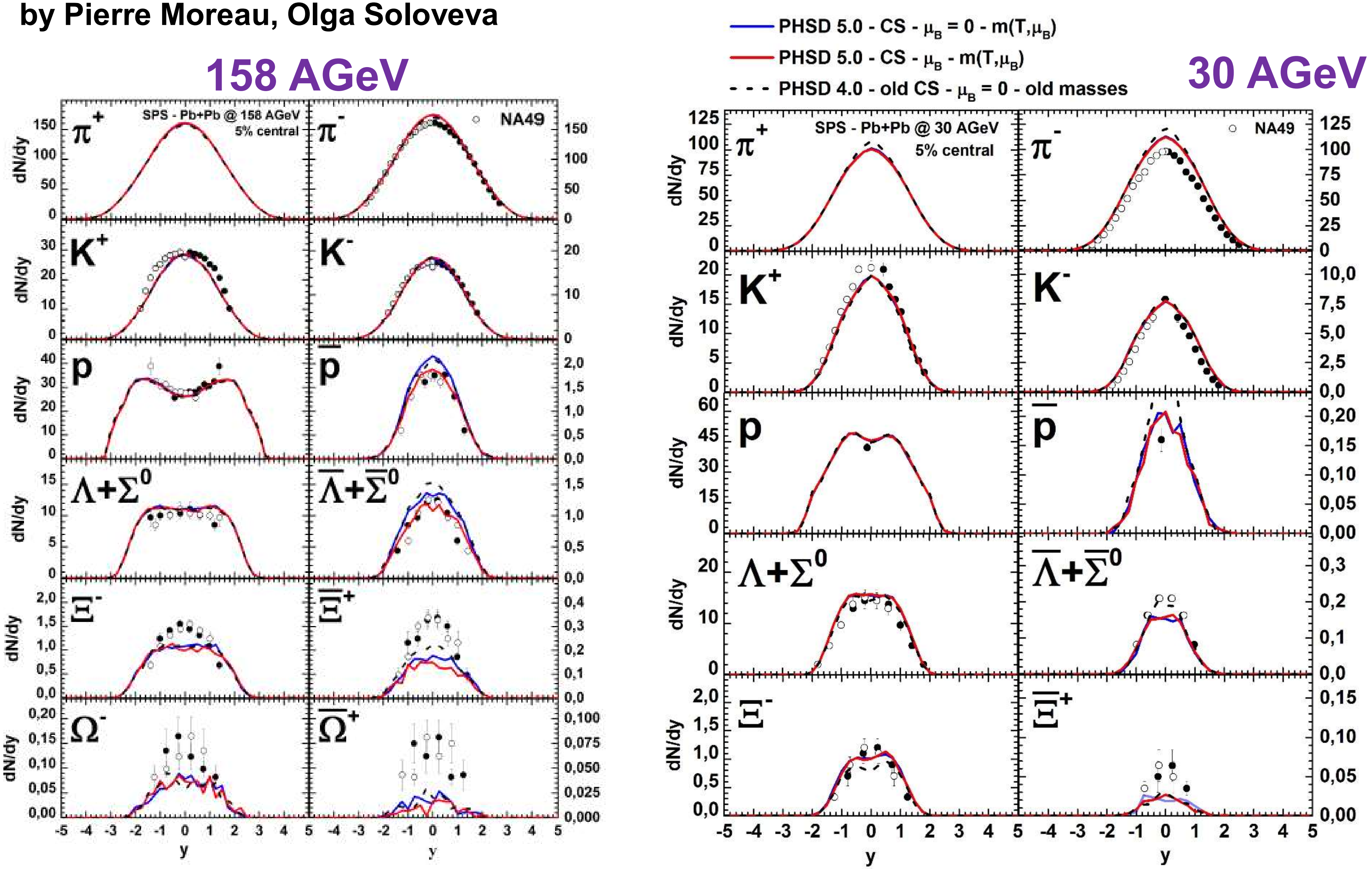

➔ Very small effect on observables when including μ_q dependence of parton masses and partonic cross sections in the PHSD

Thermodynamics of strangeness in HIC

Which parts of the phase diagram in the (T, μ_B)-plane are probed by heavy-ion collisions via the strangeness production?

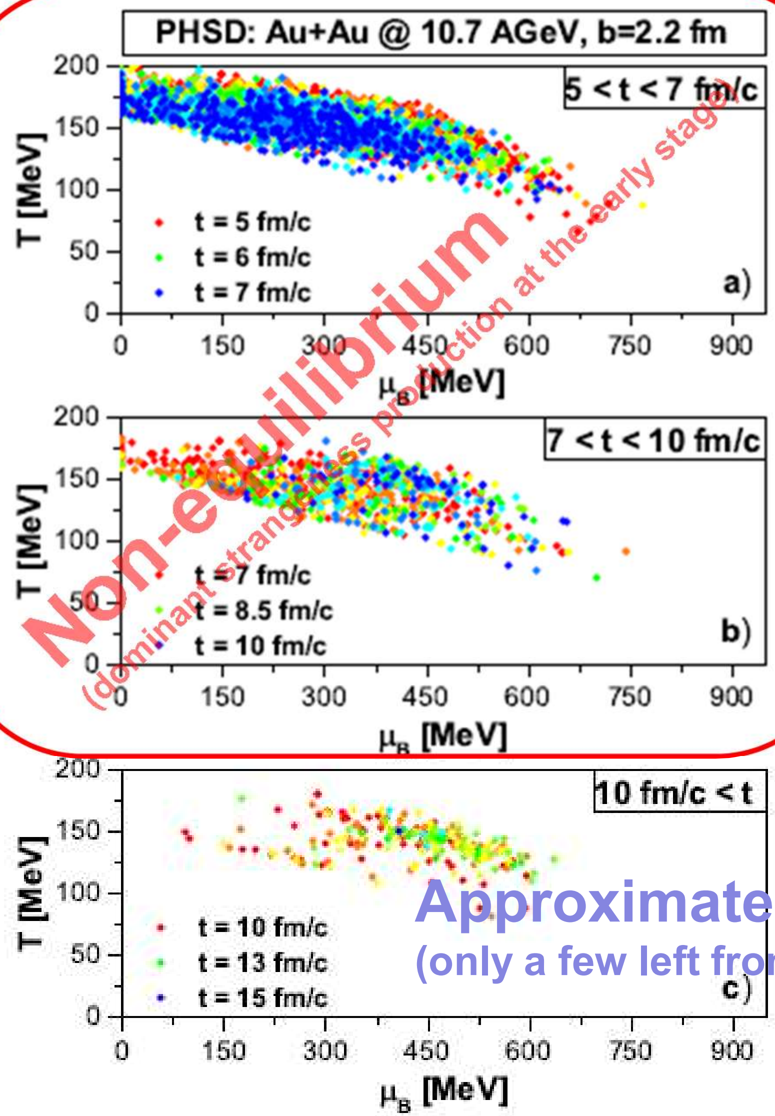

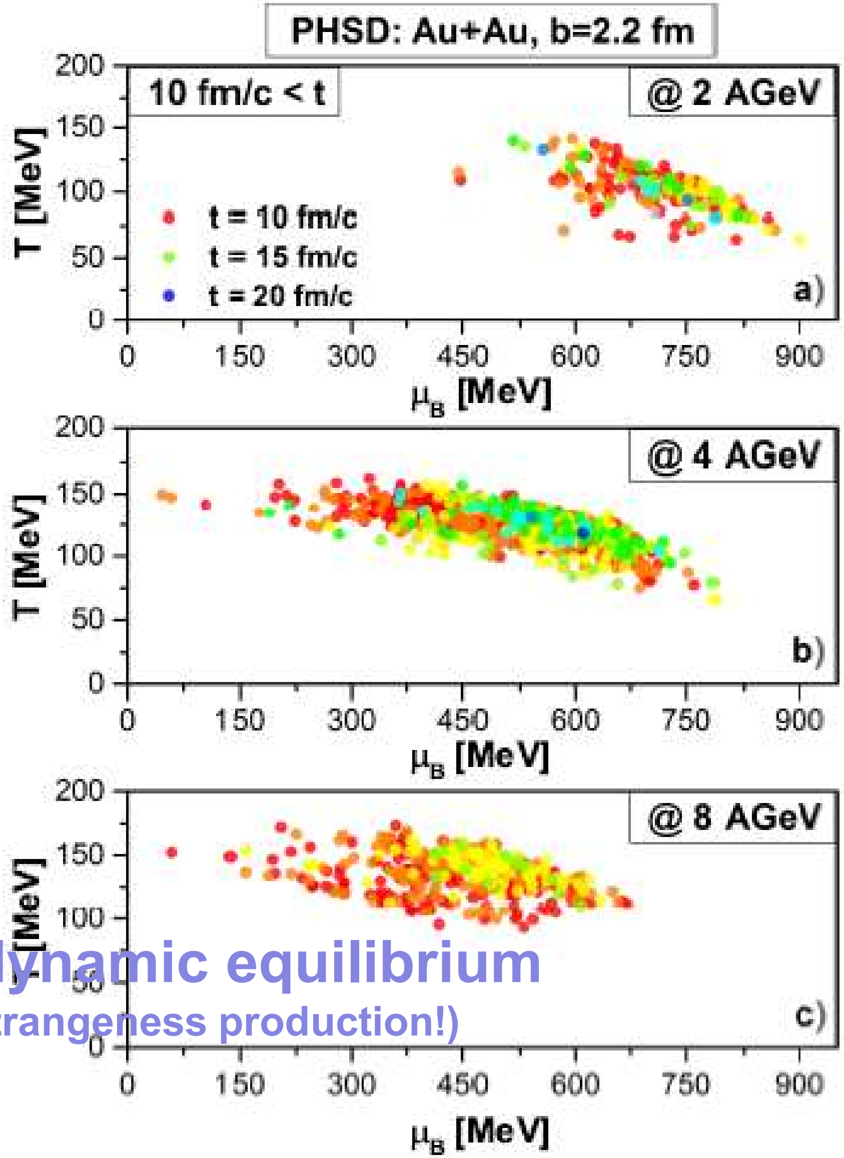

Approximate thermodynamic equilibrium
(only a few left from the total strangeness production!)

* T here corresponds to the pion, nucleon gas, i.e. the real T is smaller!

➔ the spread in T and μ_B is very large !

A. Palmese et al., PRC94 (2016) 044912 , arXiv:1607.04073

Messages from the PHSD with DQPM(T, μ_q)

- lQCD (Christian Schmidt):

> ➡ No indication for critical point, limit: $\mu_B^{\mathrm{CEP}} > 400\mathrm{MeV}$

- PHSD with the DQPM (T,μ_q) [with lQCD EoS → crossover]:
  - very small effect on observables when including μ_q dependence of parton masses and partonic cross sections in the PHSD
  - large μ_q region (where the critical point is possibly located) is accessible at low bombarding energies E_{kin} , however, the fraction of QGP decreases strongly with decreasing E_{kin}

> → Very difficult experimentally to observe a critical point /1st order phase transition!

Thanks to:

PHSD group - 2018

GSI & Frankfurt University
Elena Bratkovskaya
Pierre Moreau
Lucia Oliva
Olga Soloveva

Giessen University
Wolfgang Cassing
Taesoo Song

Thanks to Olena Linnyk
Volodya Konchakovski
Hamza Berrehrah

Thorsten Steinert
Alessia Palmese
Eduard Seifert

External Collaborations

SUBATECH, Nantes University:
Jörg Aichelin
Christoph Hartnack
Pol-Bernard Gossiaux
Marlene Nahrgang

Texas A&M University:
Che-Ming Ko

JINR, Dubna:
Viacheslav Toneev
Vadim Voronyuk
Viktor Kireev

Valencia University:
Daniel Cabrera

Barcelona University:
Laura Tolos

Duke University:
Steffen Bass

GSI
GOETHE UNIVERSITÄT FRANKFURT AM MAIN
FIAS Frankfurt Institute for Advanced Studies
HIC for FAIR Helmholtz International Center
HGS-HIRe for FAIR Helmholtz Graduate School for Hadron and Ion Research
Bundesministerium für Bildung und Forschung
DAAD
CRC-TR 211
DFG Deutsche Forschungsgemeinschaft
PHSD
JUSTUS-LIEBIG-UNIVERSITÄT GIESSEN
Subatech
TEXAS A&M UNIVERSITY
JINR
UAB Universitat Autònoma de Barcelona
Duke UNIVERSITY